A STUDY OF THE PARAMETERS CONTROLLING THE SWITCHING TIMES OF A JUNCTION TRANSISTOR OPERATING IN THE SATURATED REGION

Frederick D. Jackson

A STUDY OF THE PARAMETERS CONTROLLING THE SWITCHING TIMES OF A JUNCTION TRANSISTOR OPERATING IN THE SATURATED REGION

* * * *

Frederick D. Jackson

A STUDY OF THE PARAMETERS CONTROLLING THE SWITCHING TIMES OF A JUNCTION TRANSISTOR OPERATING IN THE SATURATED REGION

by

Frederick D. Jackson
Lieutenant, United States Navy

Submitted in partial fulfillment
of the requirements
for the degree of
MASTER OF SCIENCE
IN
ENGINEERING ELECTRONICS

United States Naval Postgraduate School
Monterey, California

1 9 5 6

This work is accepted as fulfilling

the thesis requirements for the degree of

MASTER OF SCIENCE

IN

ENGINEERING ELECTRONICS

from the

United States Naval Postgraduate School

A new era of electronics was born on July 15, 1948 when the Bell Telephone Laboratories, in an article entitled "The Transistor, A Semiconductor Triode" by J. Bardeen and W. H. Brattain, announced to the world the creation of an elementary type transistor. This first unit was a point contact transistor, not too unlike its primitive ancestor, the crystal detector, which came to the end of its day by the advent of the vacuum tube. Now, after a reign of about forty years as king, the vacuum tube faces an uncertain future.

Compared to the rather slow refinement of the vacuum tube during its early days to make it a usable device, the transistor has advanced very rapidly. After the birth of the vacuum tube, almost eight years passed before the first really successful amplifier and oscillator was demonstrated in 1915. In the same period of time, the use of the transistor has become common practice. Already commercial radios, phonographs, and audio amplifiers are available and almost every major electronic product is being designed to use transistors. This rapid advance is probably due to many reasons. One of these is that the techniques of the electronic, chemical and metallurgical sciences were well known so that the art of solid state physics was rapid in its development. A second reason for the transistor's rapid advance came in 1951 with the development of the junction transistor. The problem of noise, which to this time had presented severe limitations on transistor use, was now greatly reduced, making the use of transistors in many devices very practical and desirable.

Transistors have many advantages over vacuum tubes. They are both small and light weight. They are extremely rugged, being able to withstand shocks thousands of times greater than the force of gravity. They have a long lifetime period and require no filament power. Although their power output is presently limited to a few watts, output powers of hundreds of watts and greater are felt to be achievable.

Already the transistor has replaced the vacuum tube in many applications and shall probably continue to do so in many more. The writer, however, does not share the view of some dreamers that transistors will replace all vacuum tubes. Indeed, this should not be our aim, but rather to apply its use only where it will improve or simplify the ever growing complex science of electronics. The transistor may very possibly be the key to open the door on a completely new field of electronics and make possible the invention of devices now unknown that heretofore have been impossible to achieve by the use of vacuum tubes.

One of the fields in which transistors are expected to shine brightly in the future is the field of computers and other automatic devices. This is an ever expanding area as more and more processes are being automatized and the equipment is becoming more and more complex. It is not uncommon for the number of vacuum tubes in one equipment to range in the thousands with as many watts being used for just heater power. This alone creates large power supply requirements as well as cooling problems. In addition, the reliability is very low as the expected average time between tube failures is only a matter of minutes. The transistor provides the answer to these problems as well as making circuitry simpler and with increased efficiency. The saving

of weight in power supplies, making portable equipment much lighter, is an extremely attractive feature for the military.

Although the future of transistors seems to be extremely bright, they are not without their disadvantages. Great strides have been made in recent years, but there is much yet to do to improve the frequency range, noise factor, temperature effects, and uniformity of production. Another problem, which is unique to switching circuits, is the relatively long period of time it takes transistors to switch on and off compared to the extreme speed of vacuum tubes. Because of their great advantages, especially those of reliability and low power requirements, the use of transistors in computers and other automatic devices is extremely desirable. It is, therefore, necessary that the switching times be made as fast as possible. To obtain this, those parameters governing the switching speeds must be known so that the design engineer will know the type of unit he must build. To this end, this paper is written.

The writer wishes to express his sincere gratitude to the engineers and staff of the Semiconductor Division of the Radio Corporation of America, Harrison, New Jersey, for their cooperation and suggestions while collecting the experimental data for this paper. For their guidance in obtaining, analyzing, and presenting the data, special thanks are sent to Mr. Robert Cohen, Mr. A. Lyle Cleland, and Mr. C. Frank Wheatley of the Applications Section. The writer also wishes to gratefully acknowledge the sincere interest and assistance of Professor W. Malcolm Bauer and Professor Donald A. Stentz in the preparation of this paper.

TABLE OF CONTENTS

LIST OF ILLUSTRATIONS

TABLE OF SYMBOLS

$C_{b'c}$ - Collector capacitance to the intrinsic base

$C_{b'e}$ - Emitter diffusion capacitance to the intrinsic base

C_c - Collector capacitance (Collector to base)

C_e - Emitter capacitance (Emitter to base)

E_g - Signal generator voltage

g_m - Mutual conductance

I_{B1} - Base current the instant after the pulse is turned on

I_{B2} - Base current the instant after the pulse is turned off

I_C - Collector current

I_E - Emitter current

$r_{bb'}$ - Base lead resistance

$r_{b'e}$ - Diffusion resistance to the intrinsic base

R_g - The current generator resistance

R_L - Collector load resistance

T_f - Fall time

T_r - Rise time

T_s - Storage time

$V_{b'e}$ - Voltage from the intrinsic base to the emitter

V_{cc} - DC collector voltage

α_{cb} - Forward current gain, common emitter configuration

α_{cb}^* - Inverse current gain, common emitter configuration

α_{ce} - Forward current gain, common base configuration

α_{ce}^* - Inverse current gain, common base configuration

α_{cbfco} - Forward frequency cutoff, common emitter configuration

α_{cbfco}^* - Inverse frequency cutoff, common emitter configuration

α_{cefco} - Forward frequency cutoff, common base configuration

α_{cefco}^* - Inverse frequency cutoff, common base configuration

K - Required factor when converting from ω_{ce} to ω_{cb}

ω_{cb} - 2π times α_{cbfco}

ω_{cb}^* - 2π times α_{cbfco}^*

ω_{ce} - 2π times α_{cefco}

ω_{ce}^* - 2π times α_{cefco}^*

CHAPTER I

INTRODUCTION

1. Summary

The large signal transient response in the saturated region can be calculated using the conventional small signal parameters and equivalent circuit. (1)(2) In this paper, experimental values of rise, fall, and storage times are compared with those calculated from theory (2) and where necessary, the theory is extended to include the effects of feedback capacitance. The effects of the following parameters are to be considered using a constant current (high impedance) generator driving the unit into the saturated region: $r_{bb'}$; C_e; C_c; pulse repetition frequency; temperature; pulse amplitude; alpha; inverse alpha; alpha cutoff frequency; and inverse alpha cutoff frequency. No attempt was made to determine the effects of the external circuit parameters.

The units used consisted mostly of the TA-1576 type, an experimental high frequency unit, designed for computer work. Some commercial 2N140 types designed for converter use were used.[1] Also some shrinkage units of the TA-1576 type were used to extend the data in some cases.[2]

2. Test Circuit

The circuit used to measure the rise, fall, and storage time is shown in Fig. 1. The generator used was a TEKTRONIX Type 105 Square Wave Generator. The scope used was a TEKTRONIX Type 535. The rise and fall time characteristics of the square wave generator and the scope

[1] These consisted of units Nos. 13 to 17 of Appendix I.
[2] These consisted of units Nos. 28 to 36 of Appendix I.

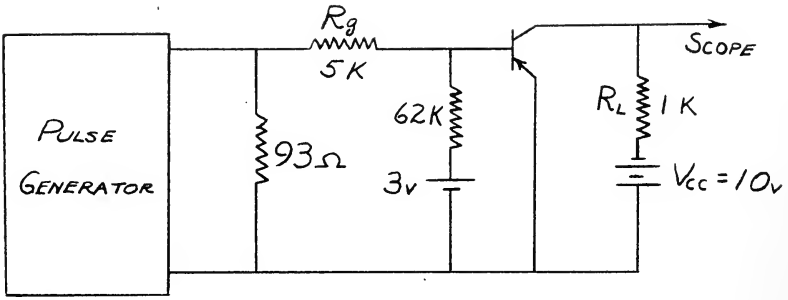

Fig. 1 Transient time test circuit.

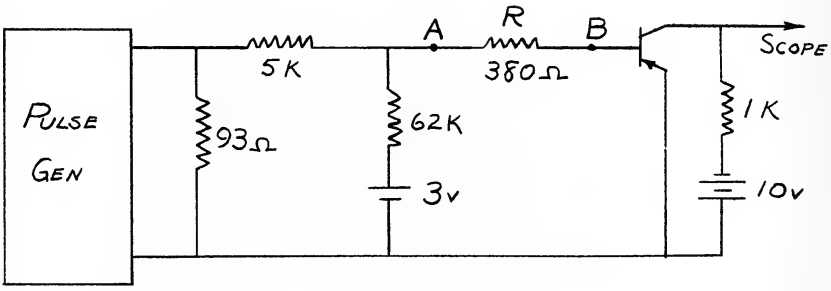

Fig. 2 Input current test circuit.

combination are shown in Fig. 3.

3. The Input Pulse Characteristics

It was desired to have the input signal a square wave block of current. Since the input resistance of the transistor, $r_{b'e} = \frac{26}{I_e \text{ (ma)}}$ ohms at 25°C (3) and is very large when the input pulse is first turned on, it was desirable to observe this input pulse to see if it was a square wave block of voltage across resistance R in Fig. 2 and thus a square wave block of current to the base lead. The circuit of Fig. 2 was used with a differential amplifier plug-in unit for the scope connected across points A and B. Photographs of these voltages are shown in Figs. 4, 5 and 6.

It is observed in Figs. 5(b) and (e) that the voltage between points A and B is a very good square wave, thus the input to the transistor base is a very good square wave block of current. The voltage waveform of point B is, therefore, proportional to the magnitude of the input impedance. Thus, Figs. 4(b), (d) and (f) can be considered as photographs of the input impedance. Notice that in Fig. 4(f) for an input signal of three ma., that the impedance remains at a lower value for a longer period of time during the "off" period than it does for an input of about one ma. as shown in Fig. 4(d). This is a result of longer storage time.

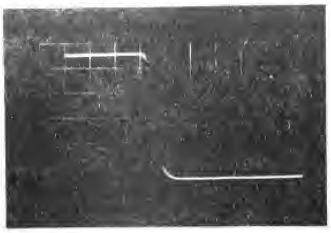

Leading Edge Eg = 5 v

Tr approx. .05μs

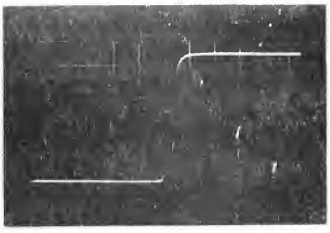

Trailing Edge Eg = 5v

Tf approx. .05μs

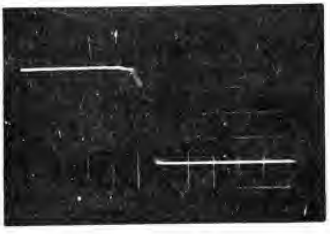

Leading Edge Eg = 15v

Tr approx. 0.1μs

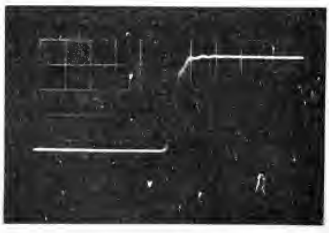

Trailing Edge Eg = 15v

Tf approx. 0.1μs

Fig. 3 Photographs showing input voltage wave form from the pulse generator for voltages of 5 and 15 volts. Time scale: 0.1μs/div.

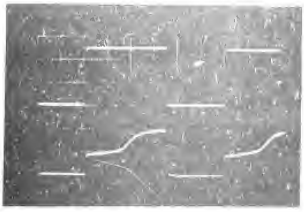

(a) Top: Input = 5v
Bottom: Pt. A
Voltage scale: 0.4v/div.
Time scale: 2μs/div.

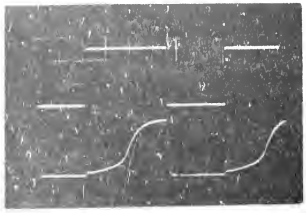

(b) Top: Input = 5v
Bottom: Pt. B
Voltage scale: 0.2v/div
Time scale: 2μs/div.

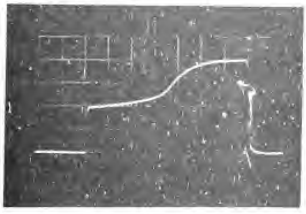

(c) Pt. A (off time) for 5v input
Voltage scale: 0.2v/div.
Time scale: 1μs/div.

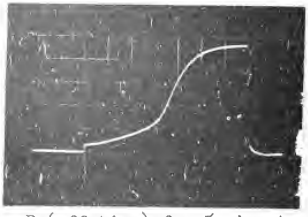

(d) Pt. B (off time) for 5v input
Voltage scale: 0.1v/div.
Time scale: 1μs/div.

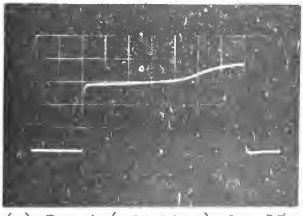

(e) Pt. A (off time) for 15v input
Voltage scale: 0.4v/div.
Time scale: 1μs/div.

(f) Pt. B (off time) for 15v input
Voltage scale: 0.1v/div.
Time scale: 1μs/div.

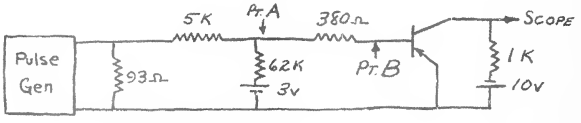

(g) Circuit Used

Fig. 4 Photographs showing the voltage variations at points A and B for unit No. 1. Input pulse: ON, 5μs; OFF, 7.2μs.

(a) [illegible]
Time [illegible]

(d) Current scale: .526 ma/div.
Time scale: 2 μs/div.
Picture upside down

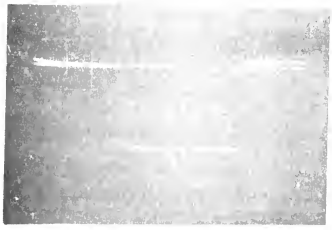

(b) Turn [illegible]
Current [illegible]/div.
Time [illegible]

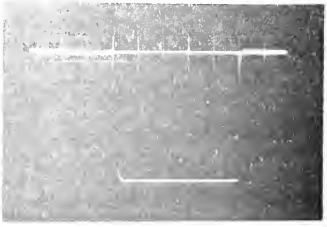

(e) Turn on time.
Current scale: .562 ma/div.
Time scale: 1 μs/cm

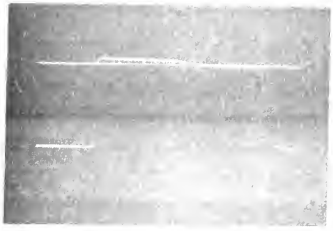

(c) Turn [illegible]
Current [illegible] ma/div.
Time [illegible]

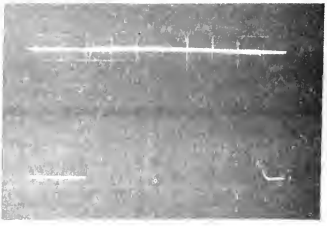

(f) Turn off time.
Current scale: .562 ma/div.
Time scale: 1 μs/div.

Fig. 5 [illegible] input current waveforms to the [illegible] Unit No. 1. (Taken using a differential [illegible] across A and B.) Input pulse: 0%, 5μs; [illegible] and (c) Eg = 5v [illegible], (e), and (f) Eg = 15v. [illegible] ence is shown.

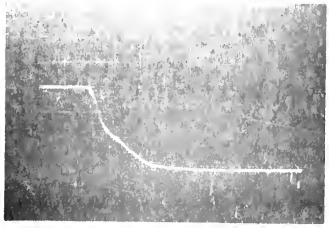

(a) Leading edge

Current scale: .263 ma/div.
Time scale: 0.1 μs/div.

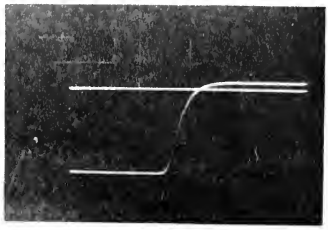

(b) Trailing edge

Current scale: .263 ma/div.
Time scale: 0.1 μs/div.

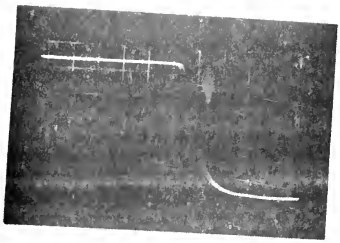

(c) Leading edge

Current scale: .526 ma/div.
Time scale: 0.1 μs/div.

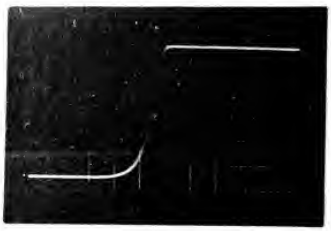

(d) Trailing edge

Current scale: .526 ma/div.
Time scale: 0.1 μs/div.

Fig. 6 Photographs showing the leading and trailing edges of the input current waveform. (a) and (b) Eg = 5 v, (c) and (d) Eg = 15v. The zero voltage reference is shown.

CHAPTER II

THEORETICAL TRANSIENT RESPONSE

1. Variations due to Transistor Parameters

The three large signal regions for the junction transistor have been defined (4) as follows:

Region I: (Collector current cutoff) Emitter and collector junctions reversed biased.

Region II: (Active) Emitter forward biased and collector reversed biased.

Region III: (Collector current saturation) Emitter and collector both forward biased.

The theoretical transient response for the transistor can be calculated in the linear region by use of the Laplace transform and the small signal parameters. For junction transistors operating in the active region, Region II, the small signal parameters are sufficiently constant that this technique can be used. If the unit is driven such that it enters Region III, carrier storage effects must be considered. Even if this is the case, the rise and fall times are measured during the period of traverse through Region II and the above method is applicable. Moll (2) has shown that where the current gain and input impedance have their short circuit values, these times for the common emitter configuration are:

$$T_r = \frac{1}{(1-\alpha_{ce})\omega_{ce}} \ln \frac{I_{B1}}{I_{B1} - .9\frac{1-\alpha_{ce}}{\alpha_{ce}} I_c} \qquad (2\text{-}1)$$

$$T_f = \frac{1}{(1-\alpha_{ce})\omega_{ce}} \ln \frac{I_C - \frac{\alpha_{ce}}{1-\alpha_{ce}} I_{B2}}{\frac{1}{10} I_C - \frac{\alpha_{ce}}{1-\alpha_{ce}} I_{B2}} \qquad (2\text{-}2)$$

$$T_s = \frac{\omega_{ce} + \omega_{ce}^*}{\omega_{ke}\omega_{ke}^*(1-\alpha_{ce}\alpha_{ce}^*)} \ln \frac{I_{B1} - I_{B2}}{I_C \frac{(1-\alpha_{ce})}{\alpha_{ce}} - I_{B2}} \qquad (2\text{-}3)$$

where I_{B1} = Base current the instant after turn-on step is applied.

I_{B2} = Base current the instant after turn-off step is applied.

I_C = Collector current at edge of Region III.

The current gain and input impedance will have their short circuit values if $\omega_{ce} R_L C_c \ll 1$. The times are defined as shown in Fig. 7.

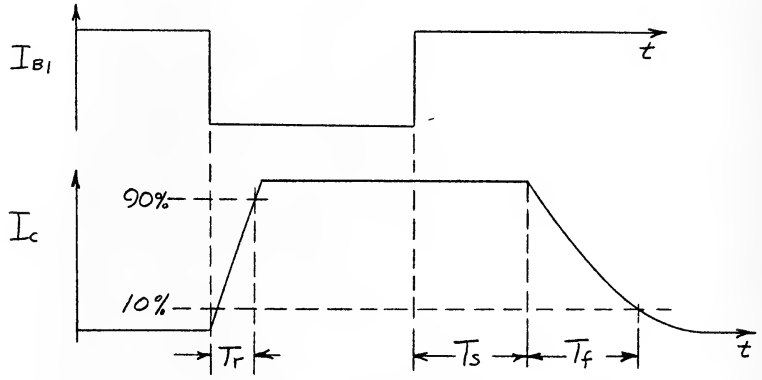

Fig. 7 Response to a large signal pulse of current.

When the unit is driven into saturation, the collector current, I_C, is limited by the external circuit, and due to the low impedance of the unit, is approximately equal to $\frac{Vcc}{R_L}$.

Using the expression $\alpha_{cb} = \frac{\alpha_{ce}}{1 - \alpha_{ce}}$ the equation (2-1) for rise time becomes:

$$T_r = \frac{\alpha_{cb}}{\omega_{ce}} \ln \frac{I_{B1}}{I_{B1} - .9\frac{I_c}{\alpha_{cb}}}$$

Let: $z = \ln \frac{I_{B1}}{I_{B1} - .9\frac{I_c}{\alpha_{cb}}}$

$$z = -\ln 1 - \frac{.9 I_c}{\alpha_{cb} I_{B1}}$$

Let: $y = \frac{.9 I_c}{\alpha_{cb} I_{B1}}$

$$I_c = \frac{V_{cc}}{R_L} = \frac{10}{1K} = 10 \text{ ma}$$

$$I_{B1(MIN)} \doteq \frac{E_g}{R_g} = \frac{5}{5K} = 1 \text{ ma}$$

$$\alpha_{cb} > 20$$

$$\therefore \; y < \frac{.9 \times 10}{20 \times 1}$$

$$y < 0.45$$

$$z = -\ln(1-y)$$

Since $y < \frac{1}{2}$

$$z = y + \frac{1}{2}y^2 + \frac{1}{3}y^3 + \cdots$$

$$= y\left[1 + \frac{1}{2}y + \frac{1}{3}y^2 + \cdots\right]$$

The third and higher terms of this series can be neglected with errors of less than 10% for $\alpha_{cb} = 20$, and $I_{B1} = 1$ ma. For higher α_{cb} units and increased drive the error is much less. Thus:

$$T_r = \frac{9}{\omega_{ce} I_{B1}}\left[1 + \frac{4.5}{\alpha_{cb} I_{B1}}\right] \qquad (2\text{-}4)$$

where $$I_{B1} = \frac{E_g}{4.71 + r_{bb'} + \frac{\alpha_{cb}}{400}} \quad ma$$

and the average value of $r_{bb'}$ for the units in use is 0.08 Kohms.

Using the expression $\omega_{ce} = \alpha_{cb}\omega_{cb}$, equation 2-4 becomes:

$$T_r = \frac{9}{\alpha_{cb}\omega_{cb} I_{B1}}\left[1 + \frac{4.5}{\alpha_{cb} I_{B1}}\right] \qquad (2\text{-}5)$$

For the larger values of α_{cb} equation 2-5 is approximately inversely proportional to $\alpha_{cb}\omega_{cb}$. Using the average value of $r_{bb'}$ in the expression for I_{B1}, the rise time as calculated by equation 2-5 for the units in use is plotted versus $\frac{1}{\alpha_{cb}\omega_{cb}}$ in Figs. 8 and 9.

Using the expression $\alpha_{cb} = \frac{\alpha_{ce}}{1-\alpha_{ce}}$ the equation 2-2 for fall time becomes:

$$T_f = \frac{\alpha_{cb}}{\omega_{ce}} \ln \frac{I_c - \alpha_{cb} I_{B2}}{.10 I_c - \alpha_{cb} I_{B2}} \qquad (2\text{-}6)$$

where, using the equivalent circuit of Fig. 11 with a constant current generator and Thevenin's Theorem

$$I_{B2} = -\frac{.228 - V_a}{4.71 + r_{bb'}} \text{ ma} \qquad (2\text{-}7)$$

$$V_a = \frac{(E_g + .247)\frac{\alpha_{cb}}{400}}{5.0 + 1.082\left(\frac{\alpha_{cb}}{400} + r_{bb'}\right)} \qquad (2\text{-}8)$$

$$I_c = 10 \text{ ma}$$

Using the average value of $r_{bb'}$, the fall time as calculated by equation 2-6 for the units in use is plotted versus $\frac{\alpha_{cb}}{\omega_{ce}}$ in Fig. 10 for constant values of α_{cb}.

Again, using the expression $\alpha_{cb} = \frac{\alpha_{ce}}{1-\alpha_{ce}}$ the equation 2-3 for storage time becomes:

$$T_s = \frac{\omega_{ce} + \omega_{ce}^*\left(1 + \alpha_{cb} + \alpha_{cb}^* + \alpha_{cb}\alpha_{cb}^*\right)}{\omega_{ce}\,\omega_{ce}^*\left(1 + \alpha_b + \alpha_b^*\right)} \ln \frac{I_{B1} - I_{B2}}{\frac{I_c}{\alpha_{cb}} - I_{B2}} \qquad (2\text{-}9)$$

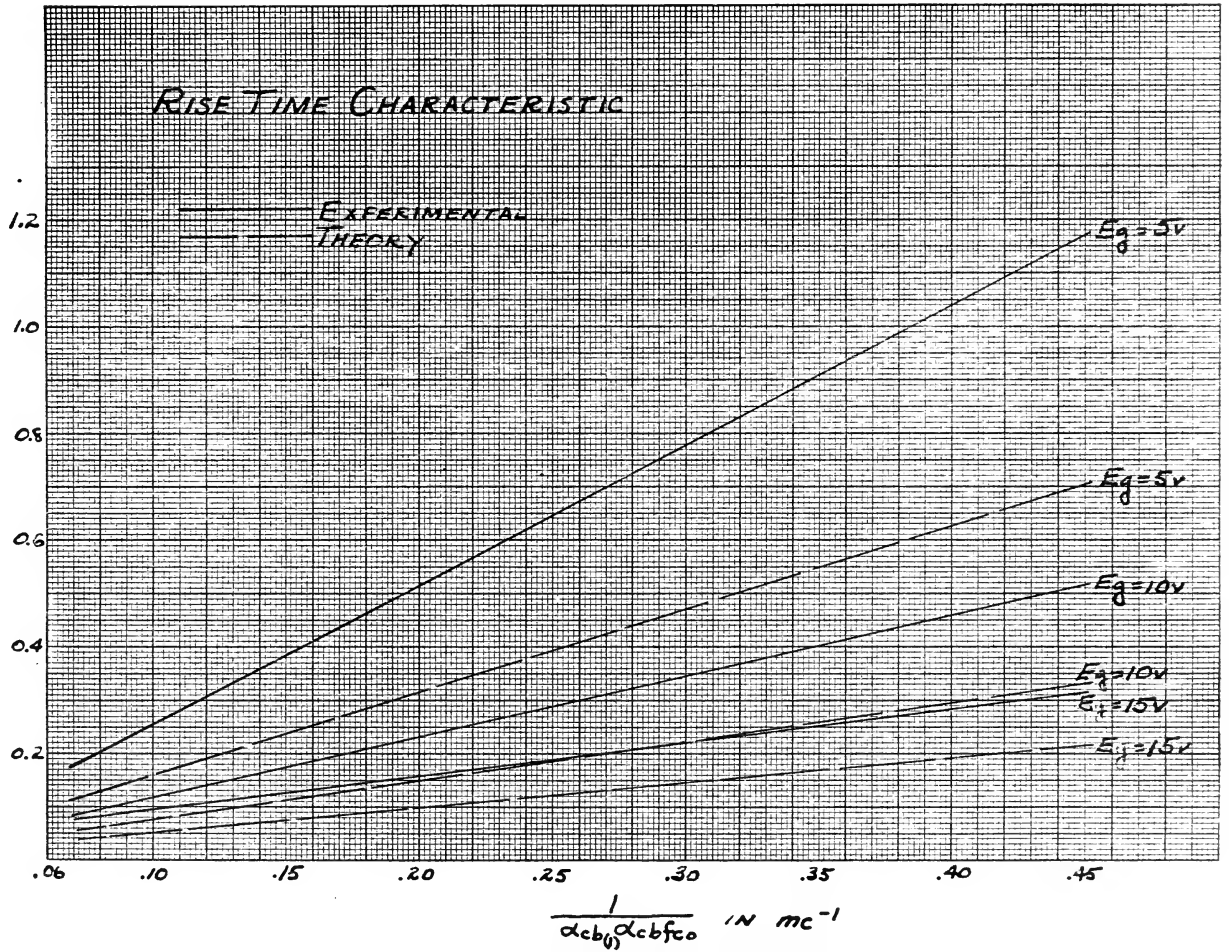
RISE TIME CHARACTERISTIC
EXPERIMENTAL
THEORY
$E_g = 5V$
$E_g = 5V$
$E_g = 10V$
$E_g = 10V$
$E_i = 15V$
$E_i = 15V$
T_R IN μS.
1.2
1.0
0.8
0.6
0.4
0.2
.06
.10
.15
.20
.25
.30
.35
.40
.45
$\frac{1}{\alpha_{cb(j)}\alpha_{cbfco}}$ IN mc^{-1}

Fig. 8

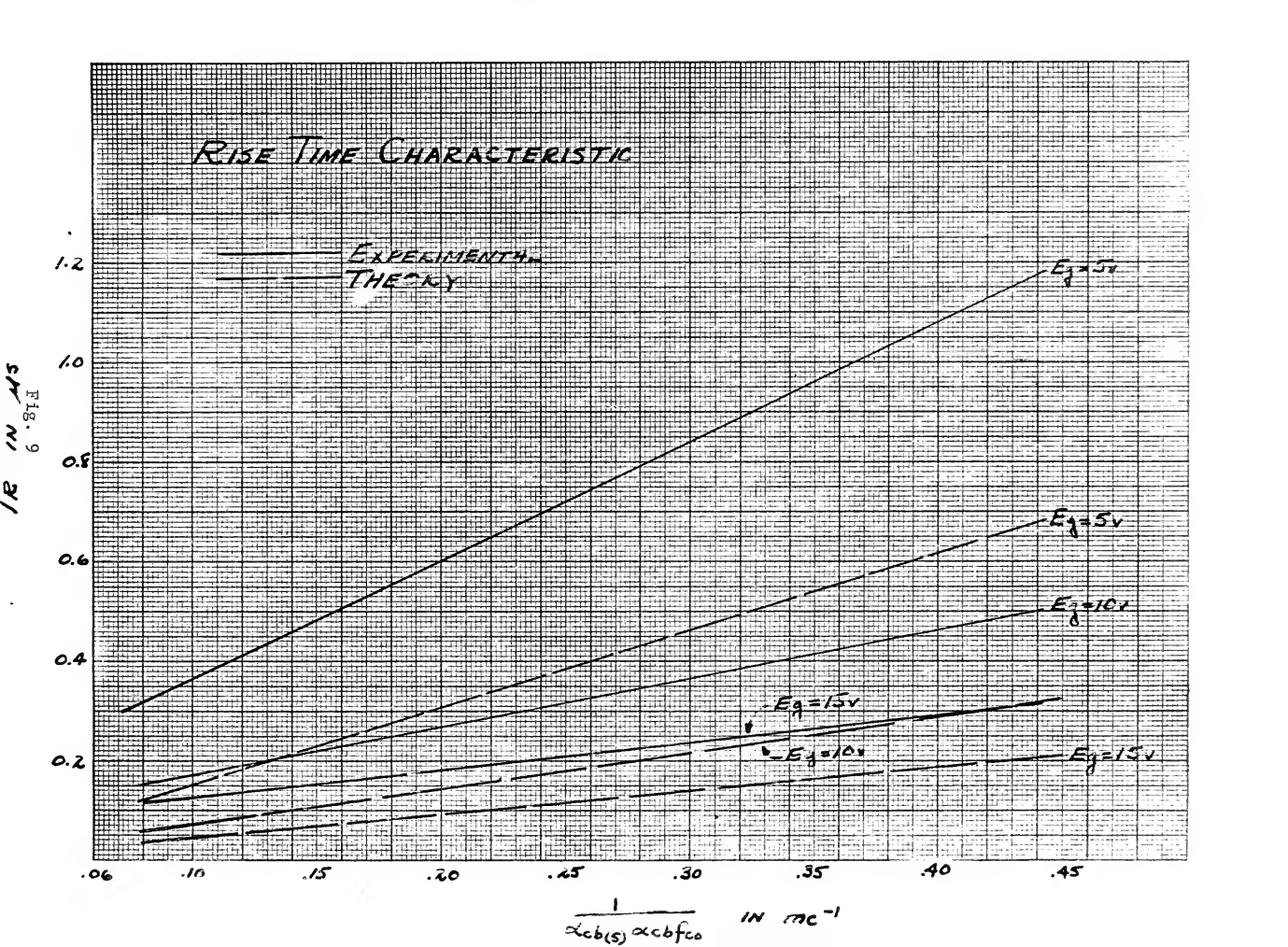
RISE TIME CHARACTERISTIC
EXPERIMENTAL
THEORY
E_g=5v
E_g=5v
E_g=10v
E_g=15v
E_g=10v
E_g=15v
1.2
1.0
0.8
0.6
0.4
0.2
.06
.10
.15
.20
.25
.30
.35
.40
.45
$\frac{1}{\alpha_{cb(s)}\alpha_{cbf_{co}}}$ IN mc^{-1}
f_R IN mc
Fig. 9

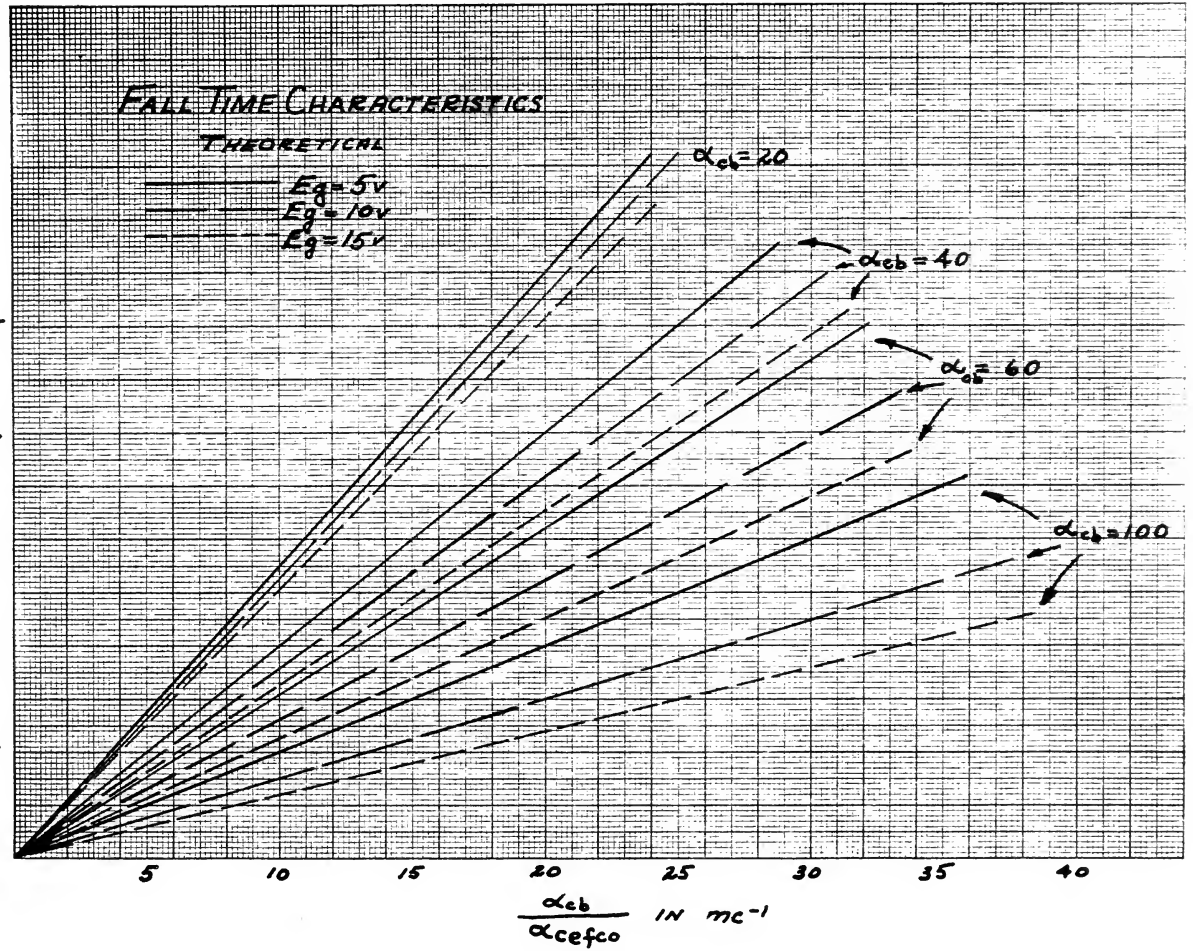
FALL TIME CHARACTERISTICS
THEORETICAL
E_g = 5v
E_g = 10v
E_g = 15v
α_{eb} = 20
α_{eb} = 40
α_{eb} = 60
α_{eb} = 100
T_f IN μs
1
2
3
4
5
5
10
15
20
25
30
35
40
$\frac{\alpha_{eb}}{\alpha_{cefco}}$ IN mc^{-1}

Fig 10

where I_{B1}, I_{B2}, and I_C are the same as before. A discussion of the plot of this theoretical equation is to follow in Chapter IV.

2. Variations due to Signal Amplitude

Signal amplitude is not a parameter that can be varied by the design of the transistor so that its consideration in this paper may seem a little out of place. It is not, however, a true curcuit parameter either. Since signal amplitude is somewhat dependent on the transistor parameters of the preceeding unit, if a transistor is being used as a driver, it is included here for completeness.

As signal amplitude is increased from five to fifteen volts, I_{B1} is increased from approximately one to three ma. It can be seen from equation 2-5 that the rise time, for large α_{cb} units, is approximately inversely proportional to I_{B1}. This decrease in rise time with an increase in drive can also be observed in Figs. 8 and 9.

Remembering that the input step voltage is a negative step, it can be seen from equations 2-7 and 2-8 that an increase in signal amplitude will cause an increase in I_{B2}. This increase in I_{B2} will cause the denominator of the logarithm in equation 2-6 to increase faster than the numerator, thus the value of the logarithm decreases and the fall time decreases. The rate at which the fall time decreases with increased input is also a function of α_{cb}. The effects of signal amplitude and α_{cb} can be seen in Fig. 10 which is a plot of the fall time, T_f, versus 2π times the time constant, $\frac{\alpha_{cb}}{\alpha_{cefco}}$.

In the storage time equation, 2-9, both I_{B1} and I_{B2} increase with increased input. This causes the numerator of the logarithm to increase

much more rapidly than the denominator, so that the value of the logarithm and thus the storage time are increased. This increase in storage time can be observed by noting the theoretical curves of Figs. 32, 33, 34 and 35. These curves will be discussed in more detail in Chapter IV.

CHAPTER III

VARIATION IN TRANSIENT RESPONSE CONSIDERING FEEDBACK

1. The Effects of Feedback Capacitance

In the development of the theory by Moll (2) the assumption was made that $\omega_{ce} C_c R_L \ll 1$. For high frequency units and reasonable values of C_c and R_L, this becomes a poor assumption. The effect of the collector capacitance, C_c, is to add feedback to the circuit and to increase the time constant, $\frac{\alpha_{cb}}{\omega_{ce}}$, in response to a pulse of base current in both the rise and fall time equations thus increasing the rise and fall times. This feedback capacitance will not affect the storage time.

2. Modification of the Theory to include Feedback Capacitance

To calculate the effect of C_c the equivalent circuit of Giacoletto (5) will be used. See Fig. 11. This circuit will be referred to frequently throughout this paper. It is convenient here to use the dual analogy of Lo, et.al. (6) so that vacuum tube techniques can be used for computing the effect of feedback capacitance. See Figs. 12(a) and 12(b). In the vacuum tube circuit, C_f can be connected across the input if it is increased by the factor (A + 1) where A is the gain and equal to $g_m R_L$. In the circuit being considered, $g_m R_L$ is much greater than 1, so that the feedback capacitance can be assumed to be across the input if increased by the factor $g_m R_L$. See Fig. 12(c). Fig. 12(d) is thus the transistor circuit, and the equivalent circuit, including R_L and the generator, becomes that of Fig. 13.

The calculation of the rise time is then as follows:

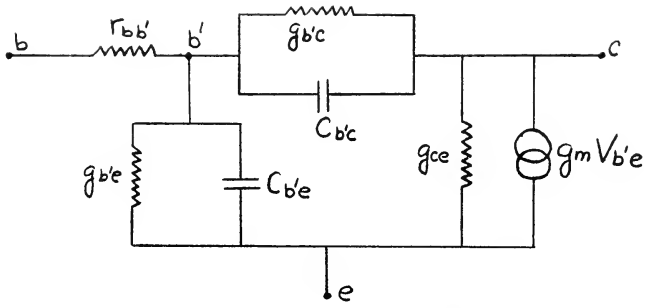

Fig. 11 The transistor equivalent circuit.

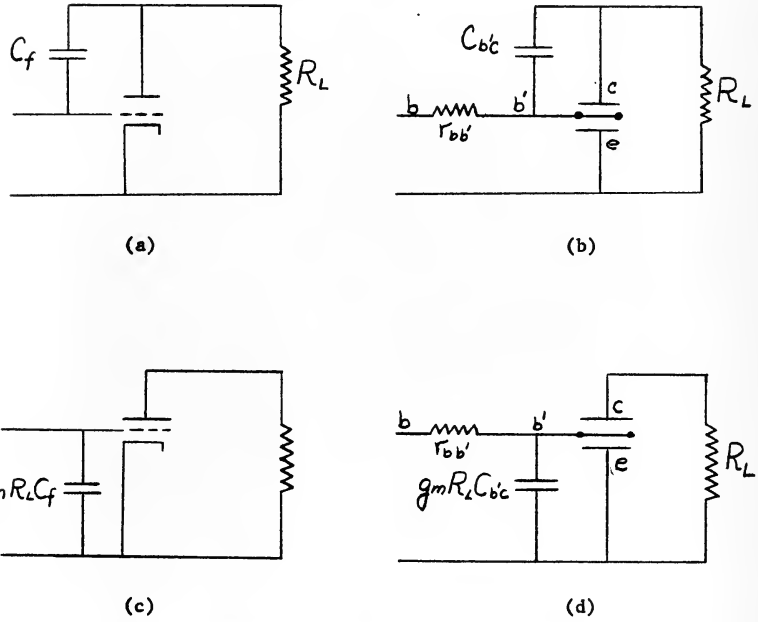

Fig. 12 The dual analogy of vacuum tubes and transistors with feedback capacitance.

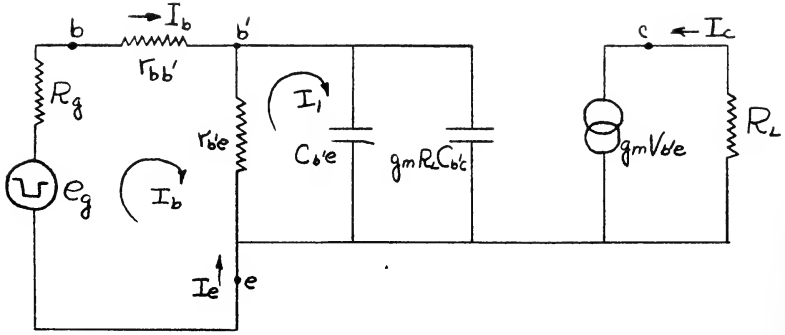

Fig. 13 Transient analysis equivalent circuit including feedback capacitance.

Let: $R = R_g + r_{bb'} + r_{b'e}$

$C = C_{b'e} + g_m R_L C_{b'c}$

$$R I_b - r_{b'e} I_1 = E_g$$

$$-r_{b'e} I_b + \left(r_{b'e} + \frac{1}{sC}\right) I_1 = 0$$

$$I_b = \frac{\begin{vmatrix} E_g & -r_{b'e} \\ 0 & r_{b'e} + \frac{1}{sC} \end{vmatrix}}{\begin{vmatrix} R & -r_{b'e} \\ -r_{b'e} & r_{b'e} + \frac{1}{sC} \end{vmatrix}}$$

$$I_b = \frac{E_g \left(r_{b'e} + \frac{1}{sC}\right)}{R r_{b'e} - r_{b'e}^2 + \frac{R}{sC}}$$

$$E_g = \frac{I_B \left[R_g r_{b'e} + r_{bb'} r_{b'e} + \frac{R}{sC} \right]}{r_{b'e} + \frac{1}{sC}}$$

$$V_{b'e} = E_g - I_b (R_g + r_{bb'})$$

$$V_{b'e} = \frac{I_b \left[R_g r_{b'e} + r_{bb'} r_{b'e} + \frac{R}{sC} \right]}{r_{b'e} + \frac{1}{sC}} - I_b \left[R_g + r_{bb'} \right]$$

$$= \frac{I_b \left[R_g r_{b'e} + r_{bb'} r_{b'e} - R_g r_{b'e} - r_{bb'} r_{b'e} + \frac{R}{sC} - \frac{R_g + r_{bb'}}{sC} \right]}{r_{b'e} + \frac{1}{sC}}$$

$$= \frac{I_b \left[\frac{r_{b'e}}{sC} \right]}{r_{b'e} + \frac{1}{sC}}$$

$$= \frac{r_{b'e} I_b}{sC r_{b'e} + 1}$$

$$V_{b'e} = \frac{r_{b'e} I_b}{s(C_{b'e} + g_m R_L C_{b'c}) r_{b'e} + 1}$$

Giacoletto (5) has shown:

$$r_{b'e} = \frac{\alpha_{cb}}{g_m}$$

From the equivalent circuit:

$$I_c = g_m V_{b'e}$$

Therefore:

$$V_{b'e} = \frac{I_c}{g_m}$$

$$\frac{I_c}{g_m} = \frac{\alpha_{cb} I_b}{g_m s(C_{b'e} r_{b'e} + g_m R_L C_{b'c} r_{b'e}) + 1}$$

Since:

$$C_{b'e} r_{b'e} = \frac{1}{\omega_{cb}}$$

$$I_c = \frac{\alpha_{cb} I_b}{s\left[\frac{1}{\omega_{cb}} + \alpha_{cb} R_L C_{b'c}\right] + 1}$$

$$I_c(s) = \frac{\alpha_{cb} \omega_{cb} I_b(s)}{s\left[1 + \alpha_{cb} \omega_{cb} R_L C_{b'c}\right] + \omega_{cb}}$$

Let: $I_b(s) = \frac{I_{B1}}{s}$

$$I_c(s) = \left[\frac{\alpha_{cb} \omega_{cb}}{1 + \alpha_{cb} \omega_{cb} R_L C_{b'c}}\right] \frac{I_{B1}}{s\left(s + \frac{\omega_{cb}}{1 + \alpha_{cb} \omega_{cb} R_L C_{b'c}}\right)}$$

$$i_c(t) = \left[\frac{\alpha_{cb}\omega_{cb} I_{B1}}{1+\alpha_{cb}\omega_{cb} R_L C_{b'c}}\right] \left[\frac{1 - e^{-\frac{\omega_{cb} t}{1+\alpha_{cb}\omega_{cb} R_L C_{b'c}}}}{\frac{\omega_{cb}}{1+\alpha_{cb}\omega_{cb} R_L C_{b'c}}}\right]$$

$$i_c(t) = I_{B1}\alpha_{cb}\left[1 - e^{-\frac{\omega_{cb} t}{1+\alpha_{cb}\omega_{cb} R_L C_{b'c}}}\right]$$

$$e^{-\frac{\omega_{cb} t}{1+\alpha_{cb}\omega_{cb} R_L C_{b'c}}} = 1 - \frac{i_c(t)}{\alpha_{cb} I_{B1}}$$

$$= \frac{\alpha_{cb} I_{B1} - i_c(t)}{\alpha_{cb} I_{B1}}$$

$$\frac{\omega_{cb} t}{1+\alpha_{cb}\omega_{cb} R_L C_{b'c}} = \ln \frac{\alpha_{cb} I_{B1}}{\alpha_{cb} I_{B1} - i_c(t)}$$

Since in the theory of Moll the rise time is the time between

$$i_c(t) = 0$$

and $$i_c(t) = 0.9 I_c$$

$$T_r = \frac{1+\alpha_{cb}\omega_{cb} R_L C_{b'c}}{\omega_{cb}} \ln \frac{I_{B1}}{I_{B1} - .9\frac{I_c}{\alpha_{cb}}} \qquad (3\text{-}1)$$

If it is assumed that $\omega_{cb} = \frac{\omega_{ce}}{\alpha_{cb}}$[1] and the capacitance $C_{b'c} = 0$, and using the expression $\alpha_{cb} = \frac{1}{1 - \alpha_{ce}}$ the equation 3-1 for rise time then reduces to that of Moll's as given by equation 2-1. Thus the affect of collector capacitance, C_c, is to increase the time constant $\frac{\alpha_{cb}}{\omega_{ce}}$ by the factor $(1 + \alpha_{cb}\omega_{cb}C_{b'c}R_L)$. The equation for fall time then becomes:

$$T_f = \frac{\alpha_{cb}}{\omega_{ce}}\left[1 + \alpha_{cb}\omega_{cb}R_L C_{b'c}\right] \ln \frac{I_c - \alpha_{cb} I_{B2}}{\frac{1}{10} I_c - \alpha_{cb} I_{B2}} \qquad (3\text{-}2)$$

3. The Effective Value of $C_{b'c}$

The question now arises as to what value should be used for $C_{b'c}$. Actually, it is impossible to measure $C_{b'c}$ but if in the measurement of C_c the base to collector current (open emitter) is limited to a few micro-amperes, as is done, the value of C_c measured is for all practical purposes equal to $C_{b'c}$.

It has been found (5)(7) that in switching applications, the effective value of C_c that must be used in switching from Region I to Region III (collector cutoff to saturation) is the value of the collector capacity, C_{co}, at the cutoff operating voltage V_{co}. When the transistor is switched from Region III to Region I, (collector saturation to cutoff) the effective collector capacity, C_c, is twice C_{co}.

4. The Transient Response including Feedback Capacitance

The rise and fall time equations, 3-1 and 3-2, now become:

[1] This is not a valid assumption as will be discussed later but must be used to obtain Moll's results.

$$T_r = \frac{1 + \alpha_{cb}\omega_{cb}R_L C_{co}}{\omega_{cb}} \ln \frac{I_{B1}}{I_{B1} - .9\frac{I_c}{\alpha_{cb}}}$$

$$T_f = \frac{\alpha_{cb}}{\omega_{ce}}\left[1 + 2\alpha_{cb}\omega_{cb}R_L C_{co}\right] \ln \frac{I_c - \alpha_{cb} I_{B2}}{\frac{1}{10} I_c - \alpha_{cb} I_{B2}}$$

The value of $\left(\frac{1}{C_{co}}\right)^2$ is a linear function of V_{cb} (5)(7). For the circuit in use, $V_{cb} = V_{co} = V_{cc}$ for all practical purposes. Thus:

$$C_{co} = \frac{\text{Constant}}{\sqrt{V_{cc}}}$$

To evaluate the constant, C_c is measured at a given test voltage. This voltage was six volts for all values of C_c measure for this paper. Therefore:

$$C_{co} = C_c\sqrt{\frac{6}{V_{cc}}}$$

Since V_{cc} = ten volts in the test circuit used,

$$C_{co} = .774C_c$$

CHAPTER IV

EXPERIMENTAL RESULTS

1. Definition of Times

The experimental rise, fall and storage times are defined in Fig. 14. Note that these are not quite the same as those defined for theory in Fig. 7. Experimental storage time should be slightly longer than that of theory, while rise and fall times should be slightly less than those of theory. The experimental definitions are taken for their ease in measurement, the exact point where the signal starts to fall being hard to see accurately on a scope. The definitions of theory were used to simplify the calculations.

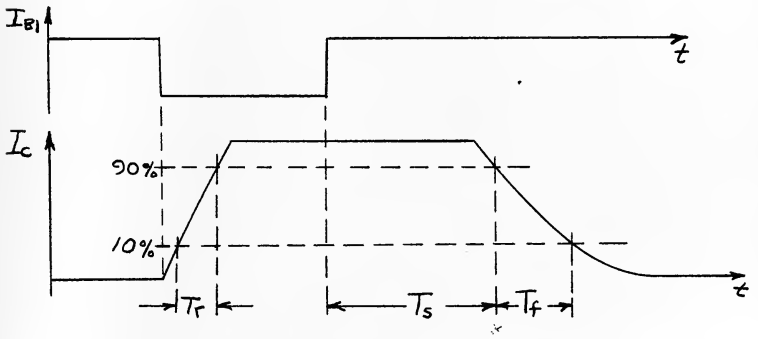

Fig. 14 Response to a pulse of current showing the definition of the time measurements used experimentally.

2. The Effects of $r_{bb'}$

The effects of $r_{bb'}$ can be measured by placing resistance in the base lead, as shown by R in Fig. 15. It is obvious that when a high

impedance circuit is used, $r_{bb'}$ + R will have little to no affect on the circuit as long as $R_g \gg r_{bb'}$ + R. This was found to be the case, for as R was increased from 0 to 400 ohms, no measurable change in the rise, fall and storage times occured.

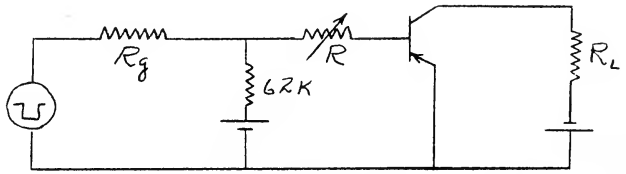

Fig. 15 Test circuit used to measure the affect of base resistance, $r_{bb'}$, by variation of resistance R.

3. The Effects of C_e and Output Capacitance of the Previous Stage

The capacitance from the point b' to the emitter in the equivalent circuit (Fig. 11) actually consists of two components. One of these, C_{Te}, is the transition junction capacitance. The second component is the $C_{b'e}$ shown in the equivalent circuit which is the diffusion capacitance. These two components are in parallel and thus add. C_{Te} is shown by Giacoletto (5) to be:

$$C_{Te} = \frac{K_e \epsilon_o}{W_e} A_e$$

where K_e = relative permittivity

ϵ_o = permittivity of free space

A_e = emitter area

W_e = emitter width

This capacitance is in the order of 10 uuf or less for the units in use. The diffusion capacitance, $C_{b'e}$, is given by

$$C_{b'e} = \lambda I_E \frac{W_b^2}{2D_p}$$

where $\lambda = \frac{q}{kT}$

I_E = emitter current

W_b = Base junction thickness

D_p = Diffusion constant of minority carriers

This capacitance is in the order of 0.05 uf for the units in use. Since C_{Te} is so much smaller than $C_{b'e}$, it is normally neglected. For this reason, a variation in C_{Te} of several uuf should not affect the rise, fall and storage times.

The exact value of C_{Te} is impossible to measure as it has one termination at b'. If, however, the base to emitter current (open collector) is limited to a few microamperes, the base to emitter capacitance measured, C_e, will very closely approximate the value of C_{Te}.

To simulate the effects of C_e, an external capacitance, C, was connected between the base and emitter, as shown in Fig. 16. The addition

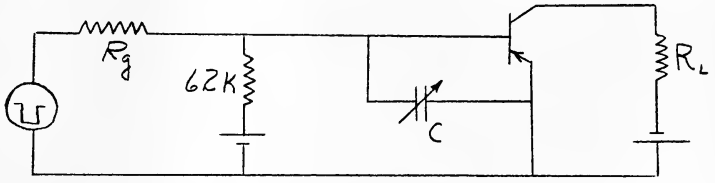

Fig. 16 Test circuit used to measure the affect of transition capacitance, C_e, by variation of capacitor C.

of this capacitance, C, is obviously not exactly the same as increasing C_e, and thus C_{Te}, but since a high impedance source is used so that $R_g \gg r_{bb'}$, the potential at b is approximately equal to that of b'. Thus

the increase in C will give almost exactly the same results as an increase in C_e.

The results of this increase in C are shown in Fig. 17 for inputs of five volts ($I_B \doteq 1$ ma.) and fifteen volts ($I_B \doteq 3$ ma) for two different units. Increasing C to about 50 uuf, which is five or six times the average value of C_e for the units used, resulted in no measurable change in the rise, fall and storage times. Thus, as was expected, the value of C_e has no affect on the rise, fall and storage times.

Using the above procedure, C could also represent the output capacitance of the previous stage. The value of C was, therefore, increased to 500 uuf. As shown in Fig. 17, there was no measurable change in the rise and storage times and only a slight increase in the fall time.

4. The Effects of C_c

As has been discussed, the value measured for C_c is for all practical purposes $C_{b'c}$. This is the transition capacitance of the collector and is shown by Giacoletto (5) to be:

$$C_{Tc} = \frac{K_c \epsilon_o}{W_c} A_c$$

where K_c = relative permittivity

ϵ_o = permittivity of free space

A_c = collector area

W_c = collector width

To simulate the effects of C_c, an external capacitance, C, was connected between the base and collector as shown in Fig. 18. As was

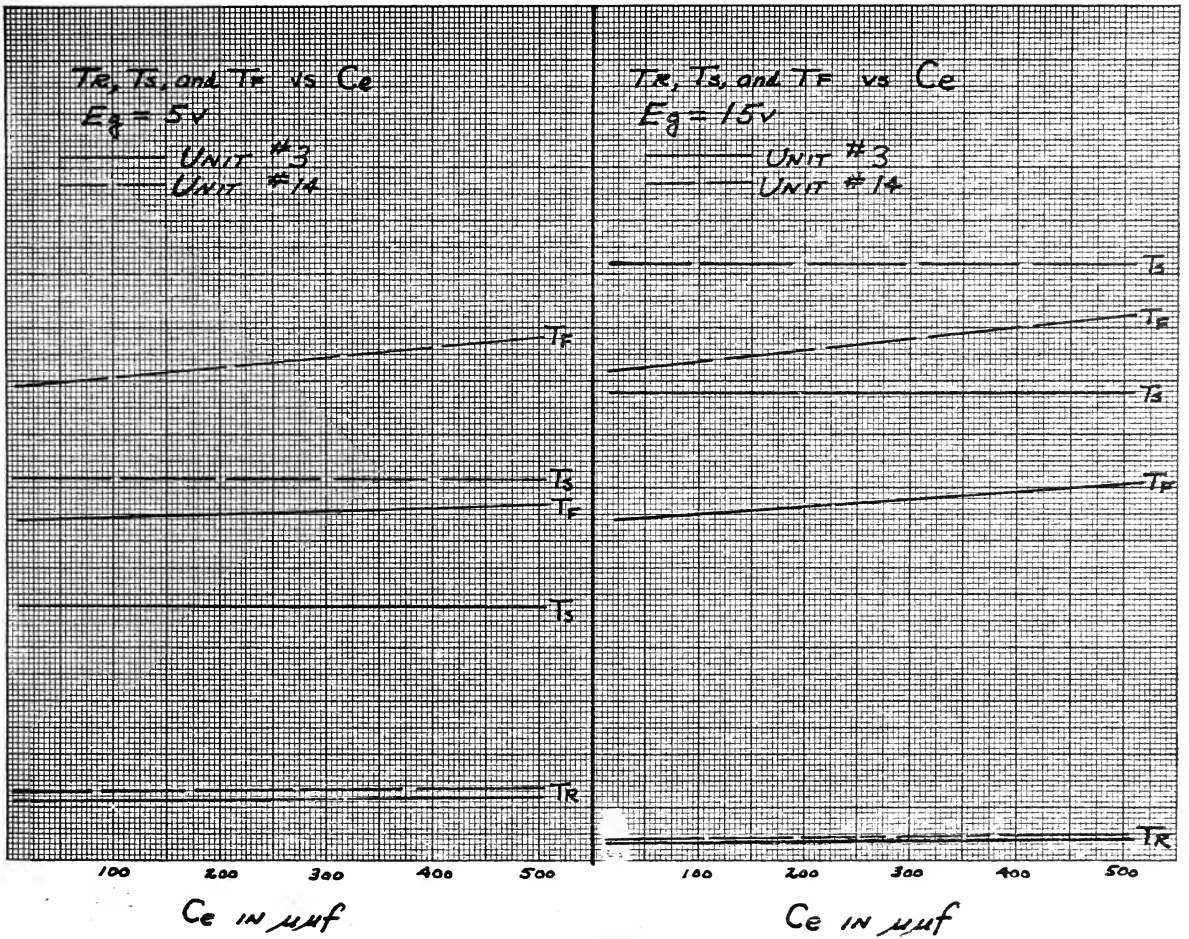

Time in μs

Fig. 17

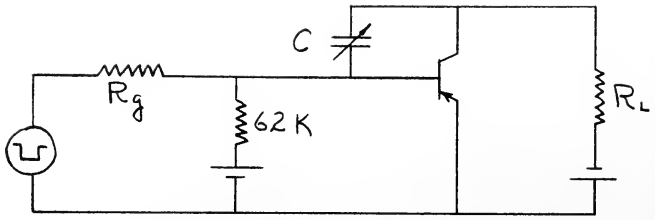

Fig. 18 Test circuit used to measure the affect of transition capacitance, C_c, by variation of C.

the case for C_e, the addition of this capacitance is not exactly the same as increasing $C_{b'c}$ as it is impossible to connect C to b', but since the potential at b' is almost exactly the same as that at b, an increase in C will give almost exactly the same results as an increase in C_c.

One limitation to this method is that $C_{b'c}$ is a function of collector current while, of course, C is not. Thus, during the period of rise and fall, $C_{b'c}$ is changing. Adding C has the affect then of adding a constant capacitance to a varying capacitance. Even though this is so, the effect is to increase $C_{b'c}$ which was desired and the results will show this effect.

As was shown in Chapter III, a change in this capacitance can substantially change the values of the rise and fall times, an increase in capacitance resulting in an increase in both the rise and fall times. In addition, equations 3-1 and 3-2 show that a linear change in $C_{b'c}$ should result in a linear change in the rise and fall times. As can be seen from Fig. 19, experimental results were as expected. The average value of $C_{b'c}$ was around twelve uuf. Increasing this by a factor of two to about 25 uuf resulted in a linear increase in both the rise and fall

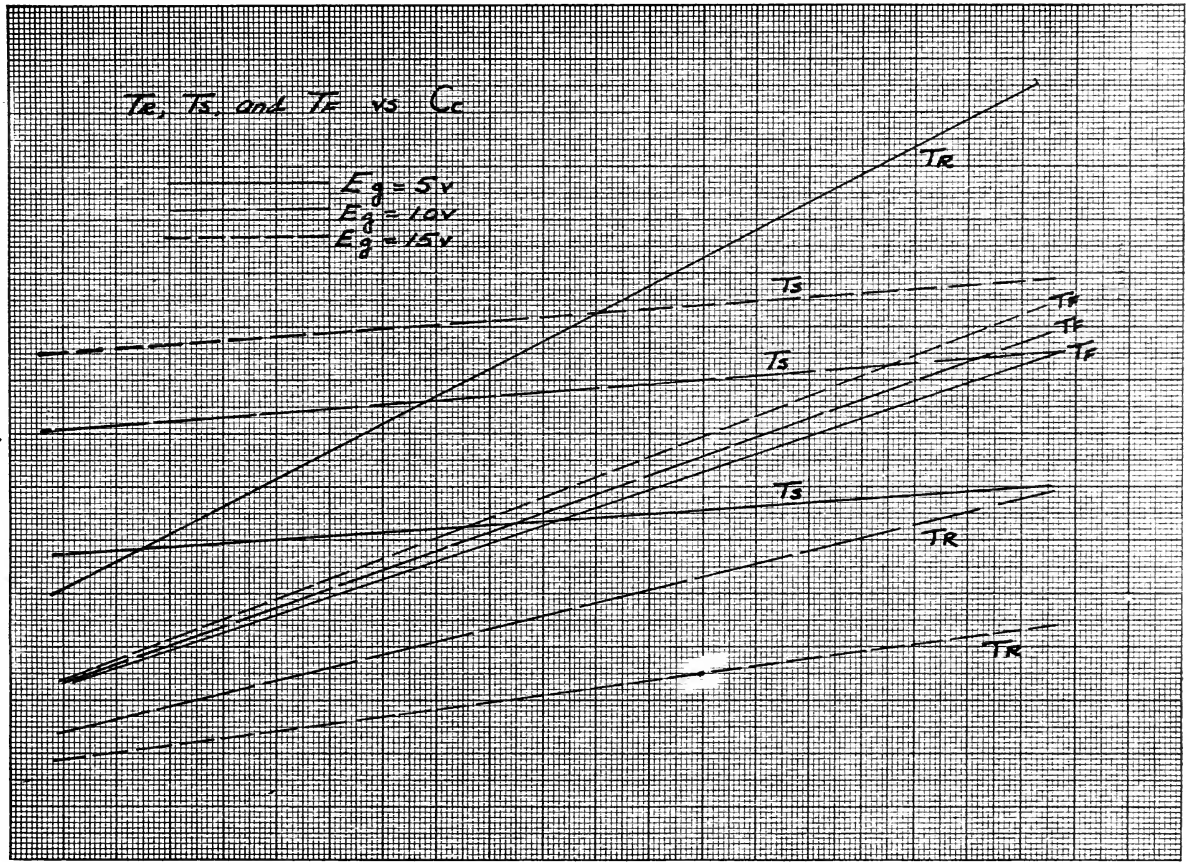
T_R, T_S, and T_F vs C_c
$E_g = 5v$
$E_g = 10v$
$E_g = 15v$
T_R
T_S
T_F
T_F
T_S
T_F
T_S
T_R
T_R
3
2
1
10
20
30
40
50
60
70
80
TIME IN MS
C_c IN MMF

Fig. 19

times with almost no increase in the storage time. To observe the effect of excessive feedback capacitance, C_c was increased to 75 uuf.

5. The Effect of Pulse Repetition Rate

The effect of the pulse repetition rate was easily obtained by changing the frequency of the pulse generator. Generally, the output of the Tektronix Square Wave Generator, used as the pulse generator, was an unsymmetrical wave of "ON" five micro-seconds and "OFF" seven micro-seconds, a pulse repetition rate of 83.3 Kc. Decreasing this to 35.7 Kc and then to 11.5 Kc resulted in no change of the rise, fall and storage times. Thus, there seems to be no lower limit to the pulse repetition rate. There is, however, an upper limit, as the "ON" pulse must be of sufficient length to permit the unit to rise to its maximum value and the "OFF" pulse must be of sufficient length to permit the unit to recover and return to Region I.

6. The Effect of Temperature

To measure the effect of temperature, it was necessary to find some method of cooling the unit at a constant rate. This was accomplished by placing the unit and a thermometer in a rubber balloon to keep them dry and then submerging them in a solution of alcohol and water. The solution was then cooled by lowering it into a thermos bottle containing liquid nitrogen keeping it above the level of the liquid so that the solution did not freeze. Good cooling control was maintained by varying the height of the solution above the liquid nitrogen. Temperatures down to -30° C were obtainable by this method. One objection to this method was that it required long leads to the unit. The error these leads caused in the measurement of rise, fall and storage time was

small, and has been subtracted from the presentation of the data.

Temperatures above room temperature were obtained by using a small heater with an attached blower.

The results of temperature change on rise, fall and storage times are shown in Figs. 20 and 21 for three different units using inputs of five volts ($I_B \doteq 1$ ma) and fifteen volts ($I_B \doteq 3$ ma). It is noted that there is only a very slight increase in the rise time while fall and storage times increase greatly with temperature.

In extensive tests made on the variation of transistor parameters with temperature (8) it has been shown that as temperature increases from -30° C to 70° C, α_{cb} increases at almost a linear rate. At the same time, $g_{b'e}$ is decreasing at almost a linear rate while $C_{b'e}$ is unaffected by temperature. The net result of these three changes with temperature is to cause ω_{ce} to decrease slightly with temperature.

Referring to equation 2-4 for the rise time, it is observed that it varies inversely with ω_{ce} when α_{cb} is large. Thus the slight decrease in ω_{ce} causes the slight increase in the rise time which is observed.

Equation 2-6 for the fall time shows that it is a function of $\frac{\alpha_{cb}}{\omega_{ce}}$. Since α_{cb} is increasing and ω_{ce} decreasing, a large increase in the fall time with increasing temperature should be observed.

As will be discussed later, the storage time is approximately a function of $\frac{\alpha_{cb}\alpha_{cb^*}}{\omega_{ce}\omega_{ce^*}}$. Since the effects of temperature on the inverse parameters will be the same as on the forward parameters, the numerator is increasing while the denominator is decreasing and thus an increase in storage time should be observed with an increase in temperature.

The results expected from knowing how the unit parameters change with

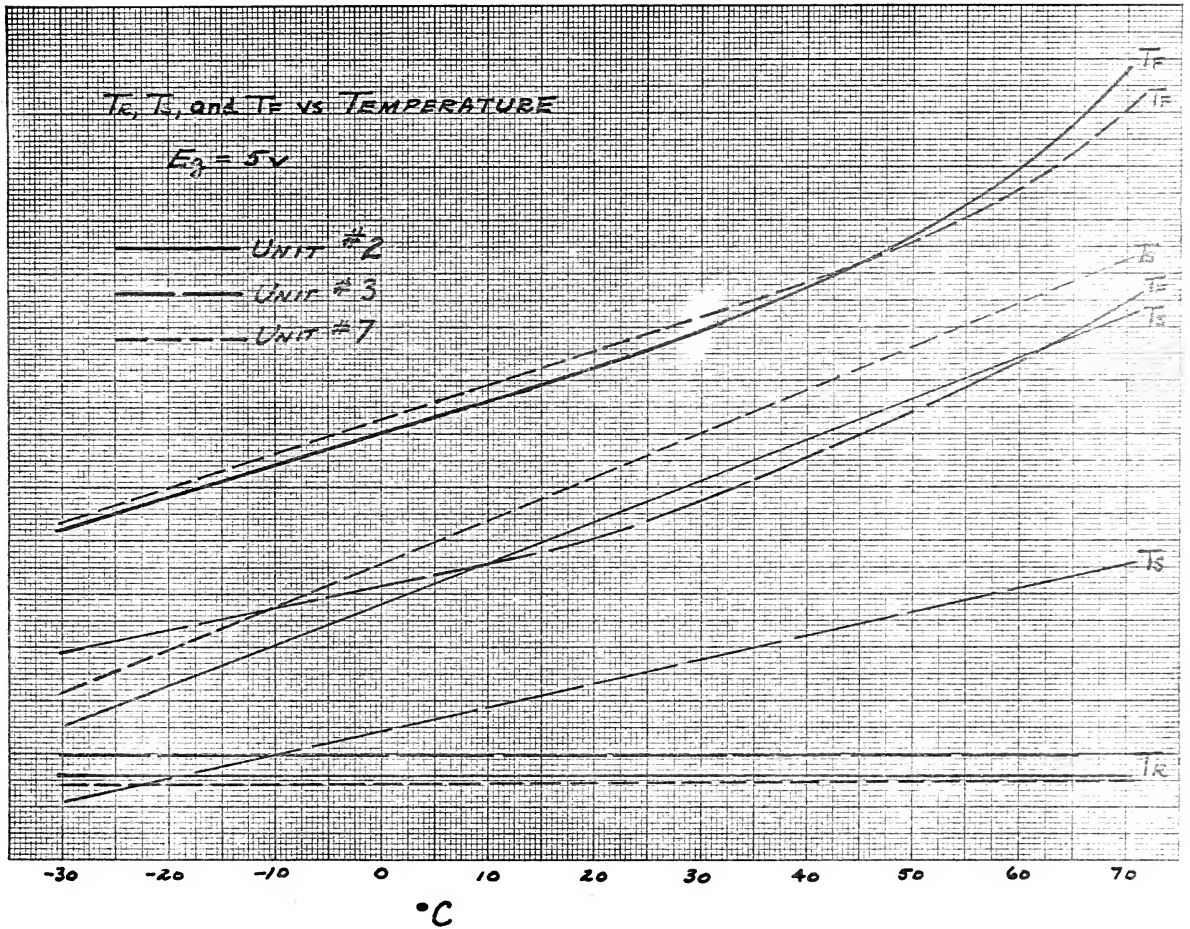
T_R, T_S, and T_F vs Temperature
E_g = 5v
Unit #2
Unit #3
Unit #7
T_F
T_F
T_S
T_S
T_R
3
2
1
-30
-20
-10
0
10
20
30
40
50
60
70
°C
Time in ms

Fig. 20

Fig. 21 Time in Min.

temperature were obtained experimentally. The bending upward of the curves at the high end of Fig. 20 is due to feedback capacitance affects. These results show that the cooler the unit, the faster will be its rise and fall times and the shorter will be the storage time. In the case of the fall and storage times, the changes are significant.

7. The Effect of Signal Amplitude

The experimental results on the effect of signal amplitude are shown most clearly on Figs. 17 and 19. In Fig. 19, which is a graph of the average results of four units, the rise time is seen to decrease with increased signal amplitude. This decrease is inversely proportional to the signal amplitude, or very nearly so, which agrees exactly with theory.

Fig. 19 also shows that the fall time increases slightly with increased amplitude. At the value of C_c = twelve uuf, which is an average value for the units in use, it can be seen that there is very little change in the fall time with increased signal amplitude. In most cases, this change was so small it could not be measured. For this reason, the fall time characteristics, Fig. 22, were plotted for an input of ten volts only. When there was a measurable change in the fall time, as occurred in a few cases, this change was very slight and the fall time was found to increase with increased signal amplitude. This is not what was predicted by the theory. The reason for this seeming contradiction, is that the theory does not account for any change in the value of α_{cb} with emitter current. The characteristic data of the transistors (Appendix I) shows that generally the α_{cb} measurements made at I_E = 5 ma are greater than those made at I_E = 1 ma. The results of tests made by

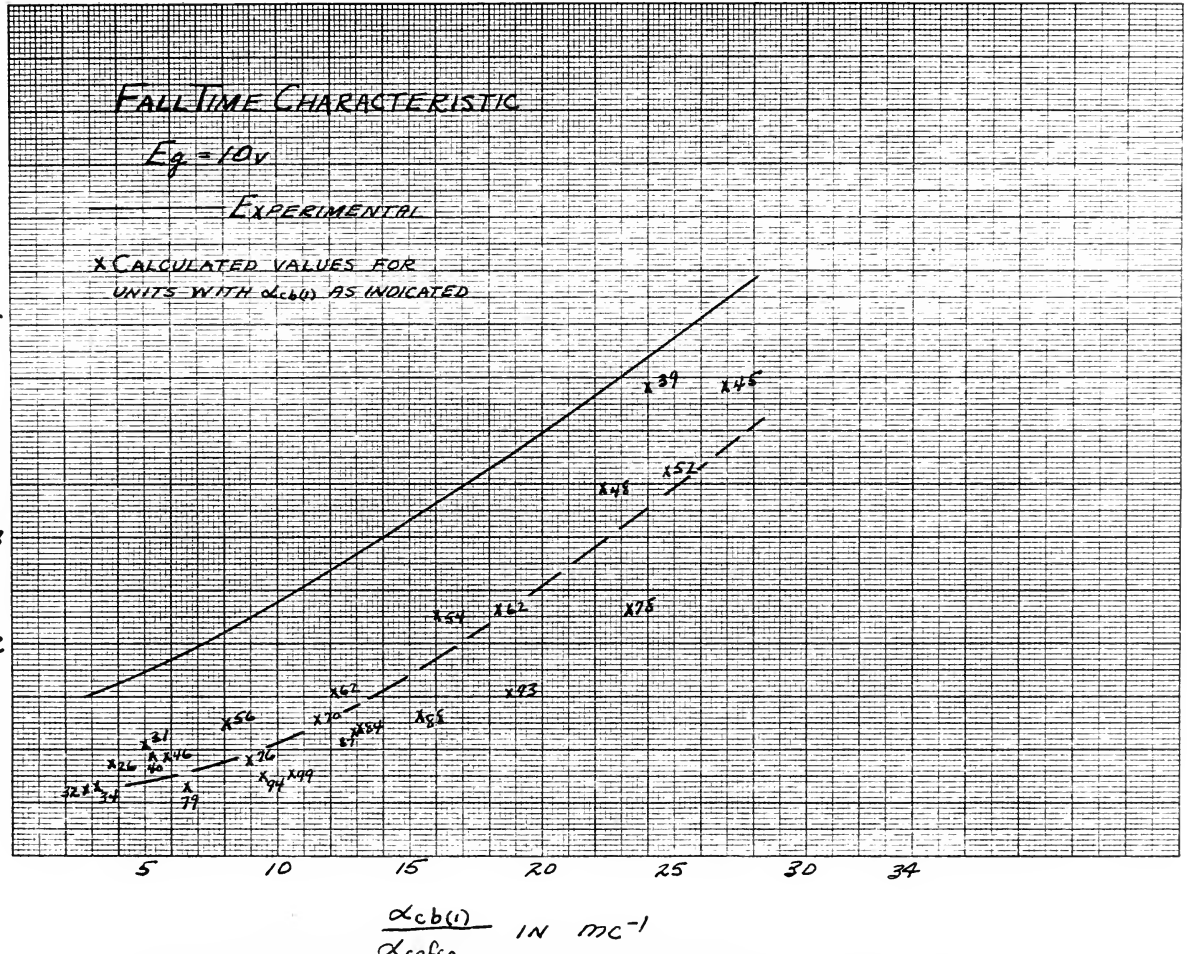
FALL TIME CHARACTERISTIC
$E_g = 10V$
EXPERIMENTAL
X CALCULATED VALUES FOR UNITS WITH $\alpha_{cb(i)}$ AS INDICATED
t_f IN μs
$\frac{\alpha_{cb(i)}}{\alpha_{cefco}}$ IN mc^{-1}
1
2
3
4
5
6
5
10
15
20
25
30
34

Fig. 22

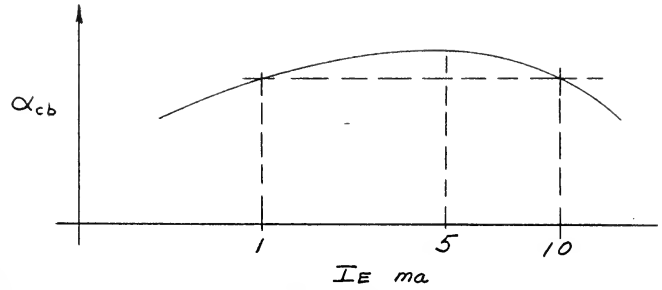

Fig. 23 Variation of α_{cb} with emitter current.

Eshelman (8), show that α_{cb} varies with emitter current approximately as shown in Fig. 23. Examination of the characteristic curves for several of the units in use indicate that the peak α_{cb} occurs at about four or five ma of emitter current. As the signal amplitude is increased, increasing the base current from about one to three ma, the emitter current is decreasing from about nine to seven ma. This means that α_{cb} is actually increasing as the signal amplitude increases. Thus, even though the value of the logarithm in the fall time equation 3-2 is decreasing with increasing signal amplitude, the value of the time constant $\frac{\alpha_{cb}\,(1 + \alpha_{cb}\omega_{cb}C_{b'c}R_L)}{\omega_{ce}}$ is increasing so that the two affects balance and there is little or no change in the fall time with temperature.

Referring again to Fig. 19, it is seen that as signal amplitude was increased, the storage time increased. This agreed with the predicted theory. The magnitude of increase in storage time with increased input signal was approximately as expected as will be discussed in the next section. Photographs of the effects of increased signal amplitude on rise, fall and storage time are shown in Fig. 24.

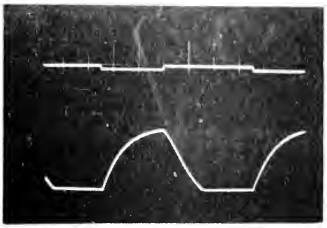

(a) Top: Input = 1.5v
Bottom: Output = 10v
Tr = 2.9 μs
Ts = 0
Tf = 2.3 μs

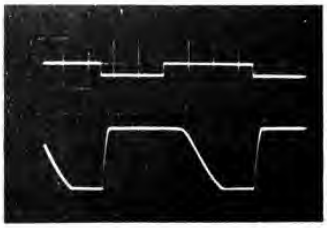

(b) Top: Input = 5v
Bottom: Output = 10v
Tr = .41 μs
Ts = 2.0 μs
Tf = 2.3 μs

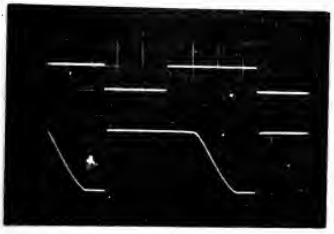

(c) Top: Input = 10v
Bottom: Output = 10v
Tr = .21 μs
Ts = 2.7 μs
Tf = 2.4 μs

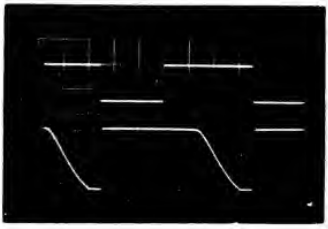

(d) Top: Input = 15v
Bottom: Output = 10v
Tr = .14 μs
Ts = 3.2 μs
Tf = 2.5 μs

Fig. 24 Photographs showing effect on rise, storage, and fall time as the input voltage is increased using unit #9. Input pulse: ON, 5μs; OFF, 7.2μs. Time scale: 2μs/div. Voltage scale: Input 10v/div; Output 4v/div.

8. The Effects of Alpha, Inverse Alpha, Frequency Cutoff and Inverse Frequency Cutoff

Experimentally, the effects of these four parameters can not be separated without an extremely large selection of units so that several units could be obtained with three of the four parameters constant. Since this large selection was not available, it was necessary to determine the effects of these four parameters concurrently.

The experimental values of rise time obtained are shown on Figs. 8 and 9, along with the theoretical values from the equation of Moll, equation 2-5. As can be seen, agreement is not at all good. Two of the main reasons for this disagreement are that: 1) Moll did not account for the affects of feedback which must be considered in this test circuit, and 2) the relationship $\omega_{ce} = \alpha_{cb}\omega_{cb}$ used is in error. The affects of feedback capacitance were discussed in Chapter III. The relationship between the common emitter frequency cutoff and the common base frequency cutoff has been discussed by numerous writers (9)(10)(11)(12)(13). Giacoletto (13) has shown that

$$\omega_{cb} \doteq \frac{1}{\alpha_{cbo}} \quad \frac{2Dp}{W_b{}^2}$$

where α_{cbo} is the low frequency value of α_{cb} and ω_{cb} is the frequency where $|\alpha_{cb}| = \frac{1}{\sqrt{2}}\alpha_{cbo}$. Haneman (12) has shown that

$$\omega_{ce} = \frac{K Dp}{W_b{}^2}$$

where K is a constant depending on the ratio of the base region width, W, and the diffusion length, L_m. The value of K ranges from 2.43 for $\frac{W}{L_m} = 0$ to 2.56 for $\frac{W}{L_m} = 0.35$. Thus

$$\frac{\omega_{ce}}{\omega_{cb}} = \alpha_{cb} \frac{K}{2}$$

In this paper a value of $K = 2.43$ was used, which assumes a base thickness of zero and thus is a little low, but the resultant error is only slight.

Figs. 25 and 26 show the Rise Time Characteristics with the above two corrections included. The theoretical curves have been corrected by the $\frac{K}{2}$ factor. So that C_{co} is not a variable in this curve, it has been assumed to be zero for the theory and its effects removed from the experimental values by normalizing. Using the value of α_{cb} measured at 1 ma of base current, the results of the theory now agree very well with those of experiment. See Fig. 25. If the value of α_{cb} measured at 5 ma of base current is used, the experimental rise times are still greater than the theoretical values. See Fig. 26. This can be explained by referring again to Fig. 23, which shows the maximum value of α_{cb} at the point where $I_E = 5$ ma. In the circuit used, I_E is between seven and nine ma. The value of α_{cb} for these emitter currents is approximately the same as for an emitter current of 1 ma. Thus, the values of α_{cb} measured at one ma is about the same as the α_{cb} for the test circuit used, while the value obtained at five ma is too large and will result in calculated values of rise time which are less than those measured.

The graph of the Fall Time Characteristics gave some unusual results. The plot of the experimental values resulted in one curve with almost a linear rise. See Fig. 22. As can be seen in Fig. 10, a family of curves was expected. In an attempt to explain the trend

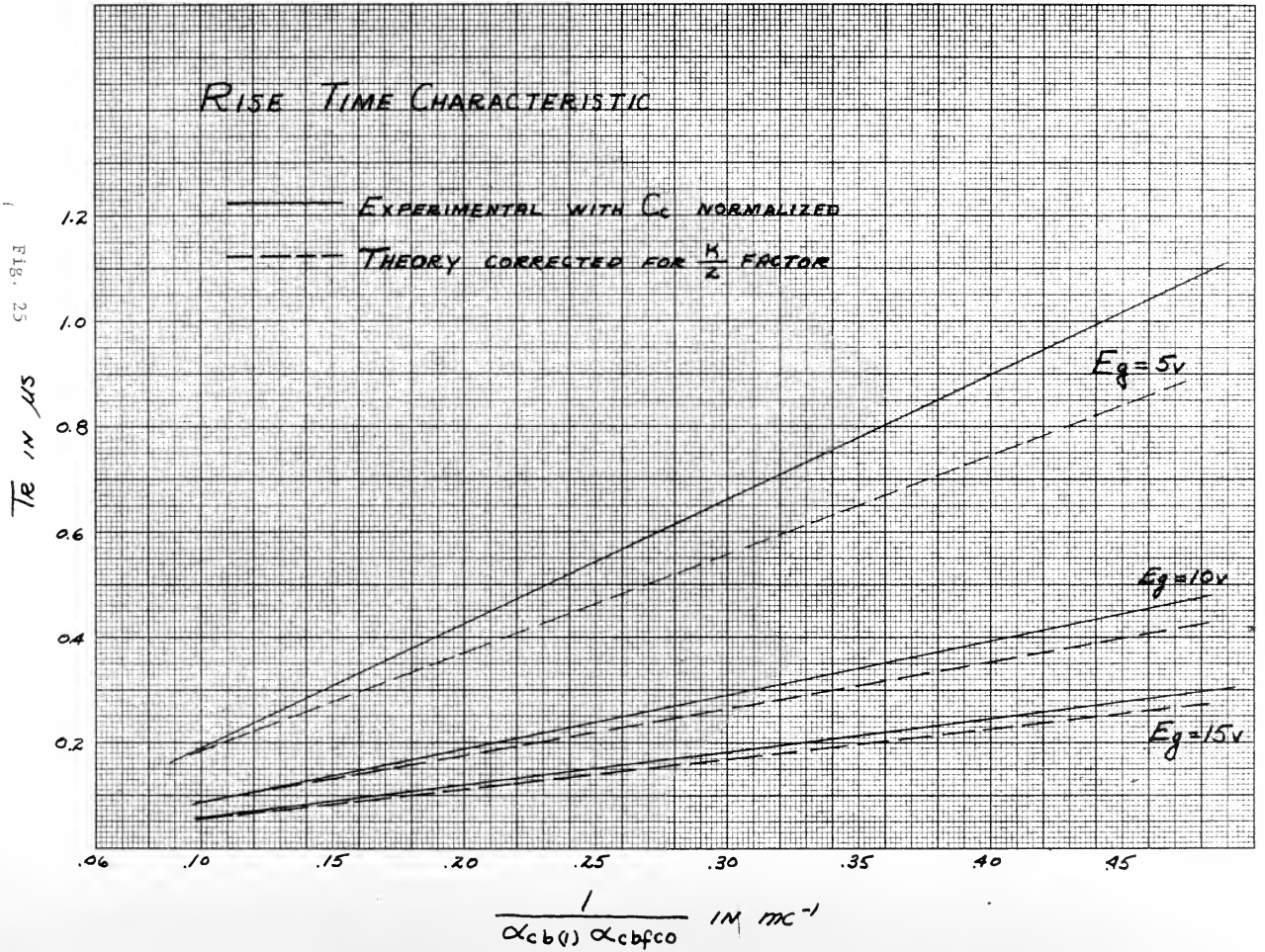
RISE TIME CHARACTERISTIC
EXPERIMENTAL WITH C_c NORMALIZED
THEORY CORRECTED FOR $\frac{K}{\Delta}$ FACTOR
$E_g = 5V$
$E_g = 10V$
$E_g = 15V$
T_e IN μS
1.2
1.0
0.8
0.6
0.4
0.2
.06
.10
.15
.20
.25
.30
.35
.40
.45
$\frac{1}{\alpha_{cb(1)}\,\alpha_{cbfco}}$ IN mc^{-1}

Fig. 25

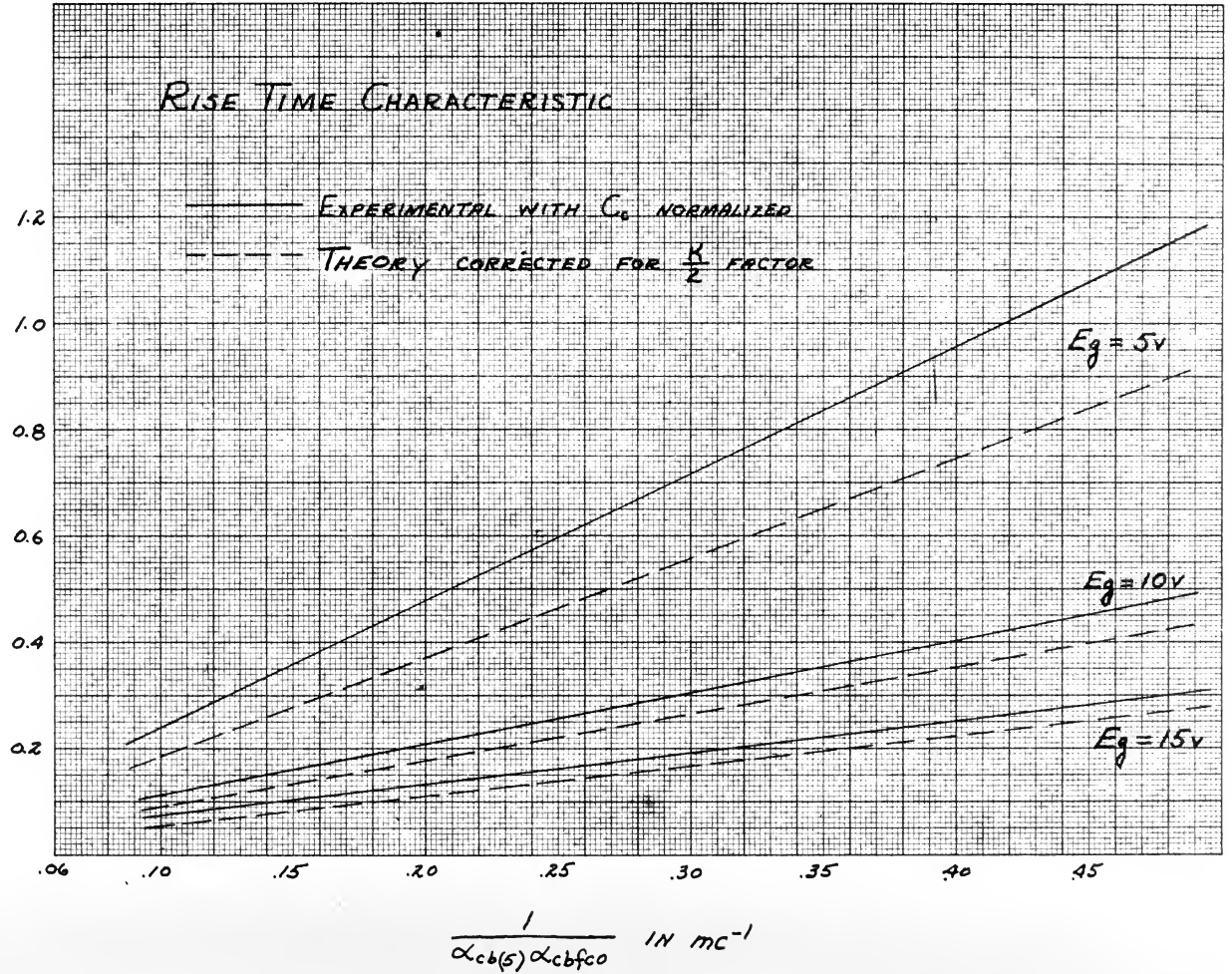
RISE TIME CHARACTERISTIC
EXPERIMENTAL WITH C_c NORMALIZED
THEORY CORRECTED FOR $\frac{K}{Z}$ FACTOR
$E_g = 5v$
$E_g = 10v$
$E_g = 15v$
1.2
1.0
0.8
0.6
0.4
0.2
.06
.10
.15
.20
.25
.30
.35
.40
.45
Tr IN μs
$\frac{1}{\alpha_{cb(s)}\alpha_{cbfco}}$ IN mc^{-1}

Fig. 26

obtained experimentally, the values of fall time were calculated for the units used to obtain the experimental curve, using the theory of Moll and the values of α_{cb} measured at one ma. The fall times obtained, with the α_{cb} used in calculation, are also shown in Fig. 22. From the plot of these points it is not too difficult to see that there is a general trend similar to that obtained experimentally, due to the choice of the units used, which choice was quite by accident. A graph showing the correlation between the experimental and theoretical fall times is shown in Fig. 27.

Using the theory developed in Chapter III, new values of fall time were calculated to include the effects of the feedback capacitance. The correlation of these calculations and experimental values of fall time are shown in Fig. 28. Using the corrected theory, good correlation results.

The correlation of the experimental values of storage time with the calculated values using the theory of Moll is shown in Figs. 29, 30 and 31. Considering the difference in the definitions of storage time of the theory and those measured, as shown in Figs. 7 and 14, it is seen that the experimental storage time should always be greater and not necessarily by a constant amount. The results in Figs. 29, 30 and 31 thus, in general, show fairly good correlation between theory and experiment. The equation used to calculate the theory, equation 2-9, is, however, quite cumbersome and the effects of the four parameters involved is not too evident by inspection. It was thus attempted to determine the effects of each of the four parameters and to determine a simpler empirical equation that might be of more value to the unit designer.

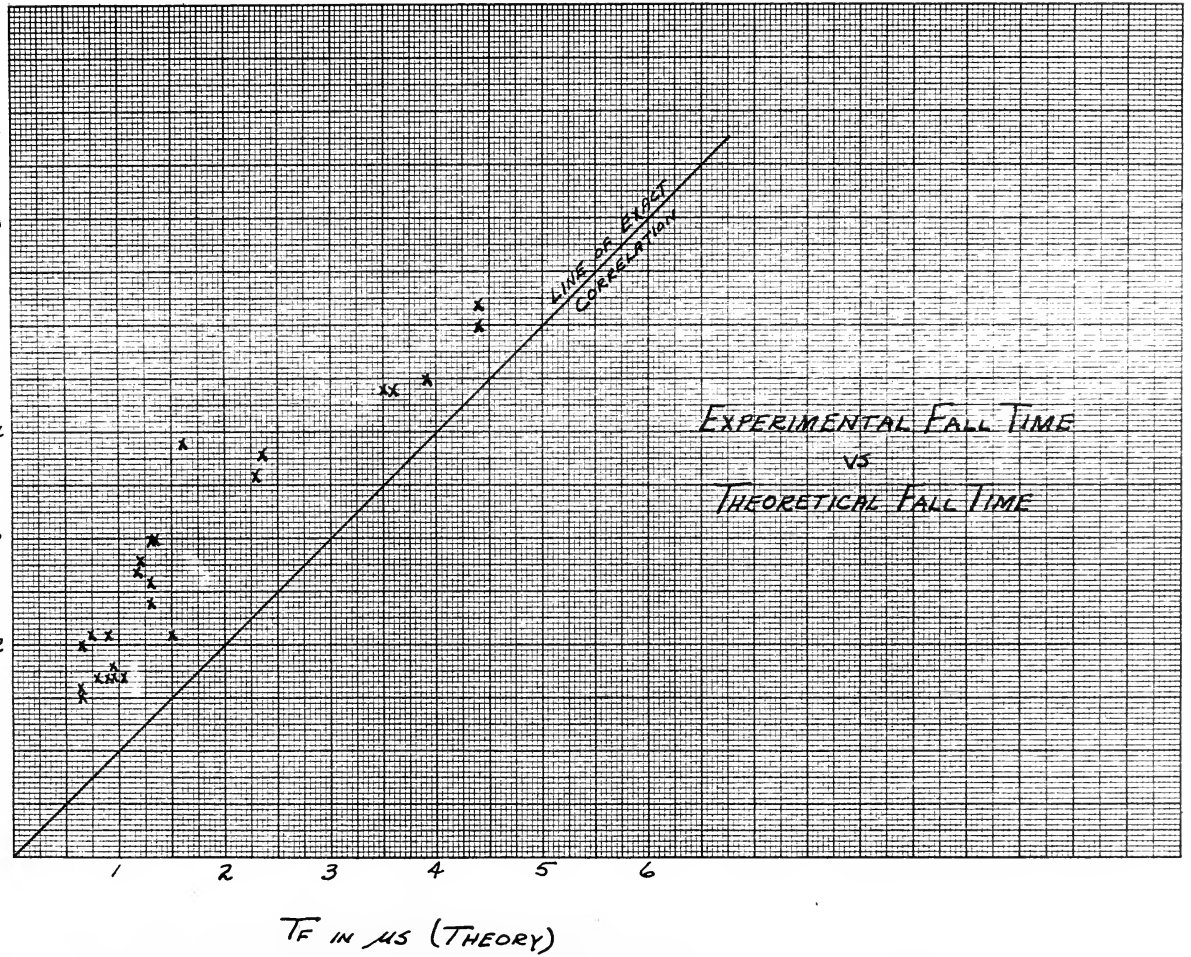
EXPERIMENTAL FALL TIME
VS
THEORETICAL FALL TIME
LINE OF EXACT CORRELATION
TF IN μS (EXPERIMENTAL)
TF IN μS (THEORY)
1
2
3
4
5
6

Fig. 27

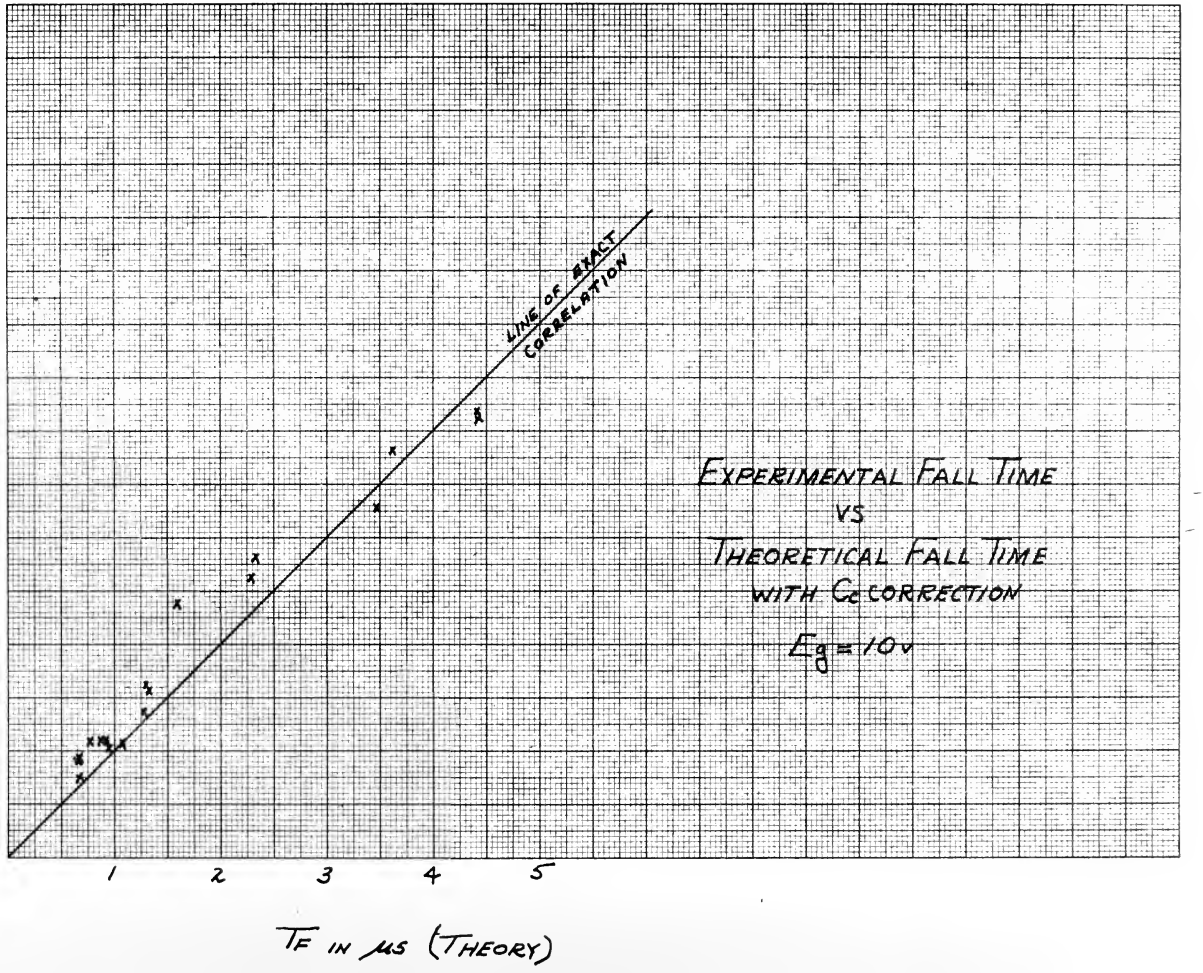
LINE OF EXACT CORRELATION
EXPERIMENTAL FALL TIME
VS
THEORETICAL FALL TIME
WITH C_c CORRECTION
$E_g = 10v$
TF IN μs (EXPERIMENTAL)
TF IN μs (THEORY)
1
2
3
4
5

Fig. 28

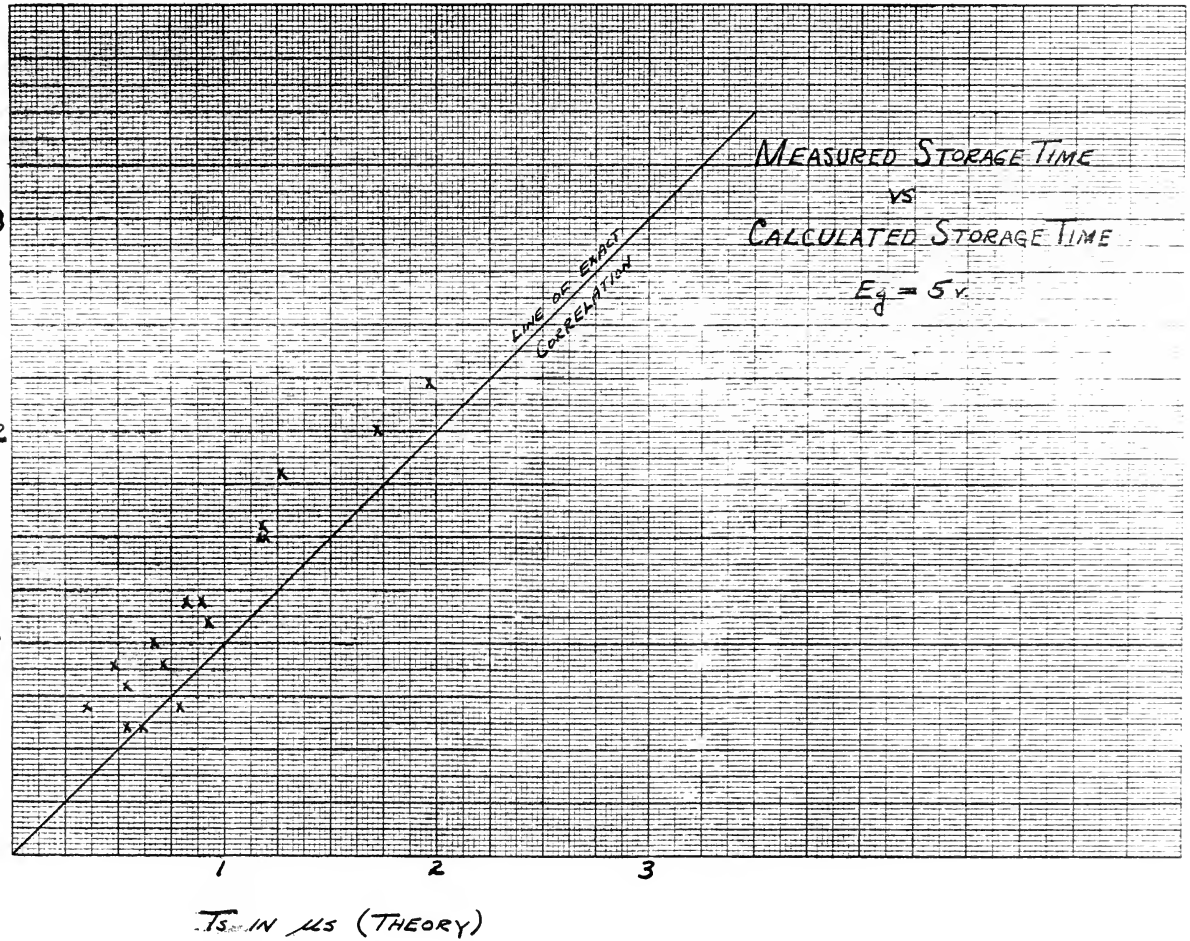
MEASURED STORAGE TIME
VS
CALCULATED STORAGE TIME
$E_g = 5$ V.
LINE OF EXACT CORRELATION
T_S IN μs (EXPERIMENTAL)
T_S IN μs (THEORY)
1
2
3

Fig. 29

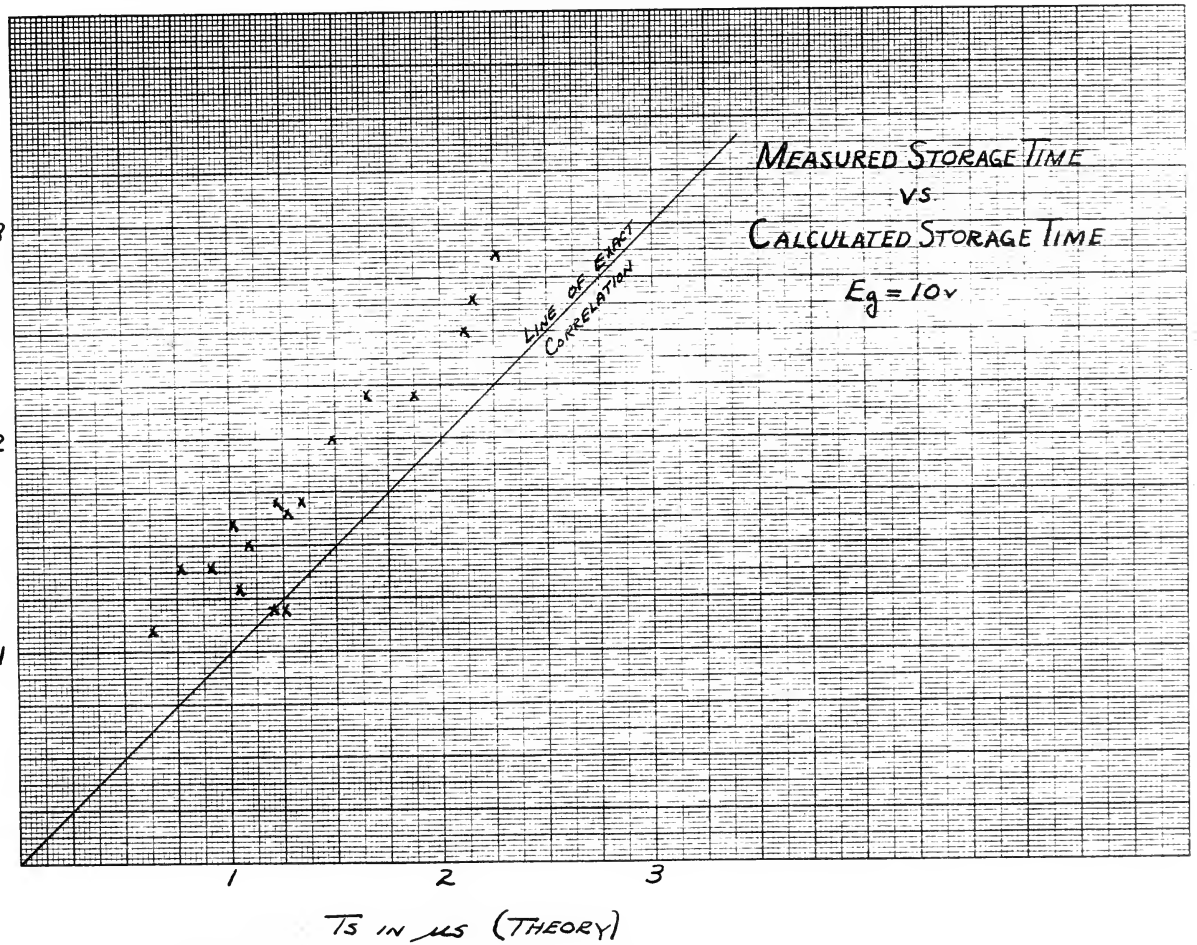
MEASURED STORAGE TIME
VS
CALCULATED STORAGE TIME
$E_g = 10v$
LINE OF EXACT CORRELATION
T_S IN μs (EXPERIMENTAL)
T_S IN μs (THEORY)
1
2
3

Fig. 30

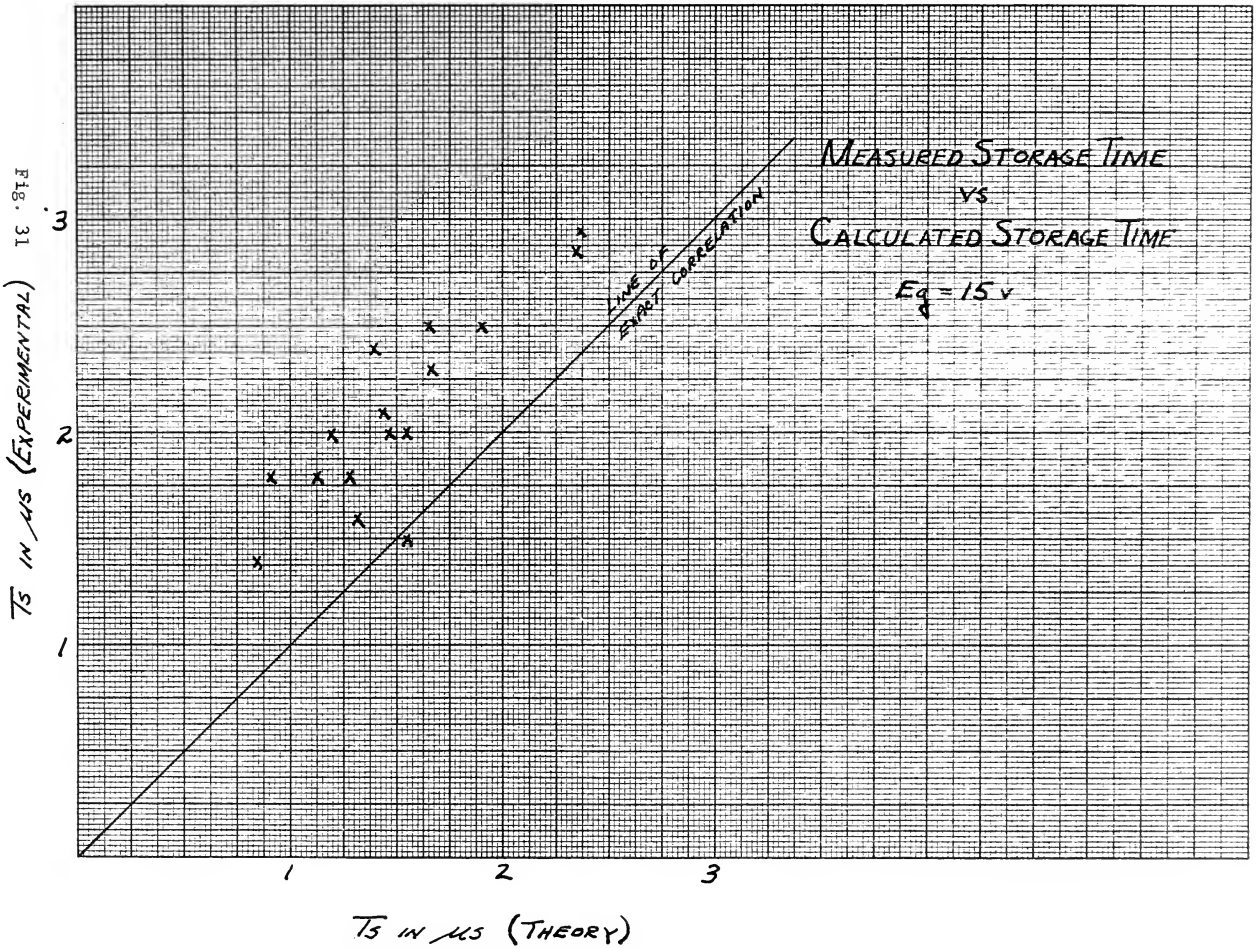
MEASURED STORAGE TIME
VS
CALCULATED STORAGE TIME
Eq = 15 v
LINE OF EXACT CORRELATION
TS IN μS (EXPERIMENTAL)
TS IN μS (THEORY)
1
2
3
1
2
3

Fig. 31

To accomplish this, those units which passed the present tentative RCA computer specifications were selected and the average value of the four parameters, alpha, inverse alpha, frequency cutoff, and inverse frequency cutoff was determined. These average values were: $\alpha_{cb} = 58$; $\alpha_{cb}^* = 7.8$; $\alpha_{cefco} = 8.6$ mc; $\alpha_{cefco}^* = 2.0$ mc. Holding three of these parameters constant at the average value, the fourth was varied and the storage time as a function of each of the four parameters are shown in Figs. 32, 33, 34 and 35 for inputs of five volts ($I_B \doteq 1$ ma) and fifteen volts ($I_B \doteq 3$ ma). From these plots it was seen that storage time was approximately a linear function of α_{cb} and α_{cb}^* and an inverse function of α_{cefco} and α_{cefco}^*. Thus, the ratio $\frac{\alpha_{cb}\alpha_{cb}^*}{\alpha_{cefco}\alpha_{cefco}^*}$ was formed and the fourth root taken to again reduce the function to a linear function. The experimental value of storage time was then plotted versus this factor for each unit for each value of input signal amplitude. The results were three straight lines each intersecting the zero time axis at 0.8 and each having a slope of $\frac{E_g + 11}{16}$. See Fig. 36. The emirical equation was then formed

$$T_s = \frac{E_g + 11}{16}\left[\sqrt[4]{\frac{\alpha_{cb}\,\alpha_{cb}^*}{\alpha_{cefco}\,\alpha_{cefco}^*}} - 0.8\right]$$

Again, the values of α_{cb} measured at one ma were used.

Using this empirical equation, the values of storage time as a function of each of the four parameters, keeping three at a time constant as before, were determined and the results are shown in Figs. 32, 33, 34 and 35. The correlation between the experimental storage time and the empirical values for each unit is shown in Figs. 37, 38 and 39. These

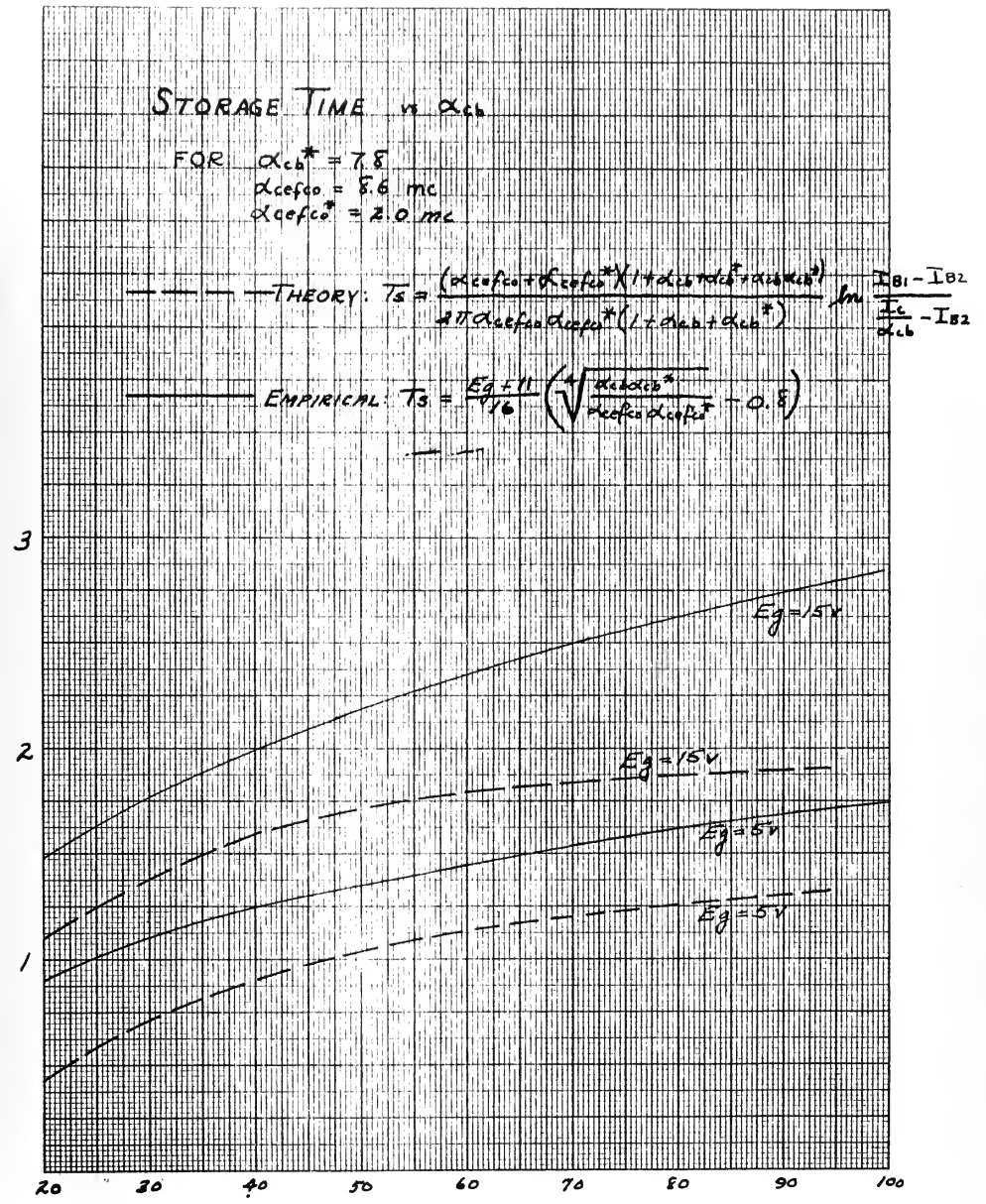

Fig. 32 $\alpha_{cb(1)}$

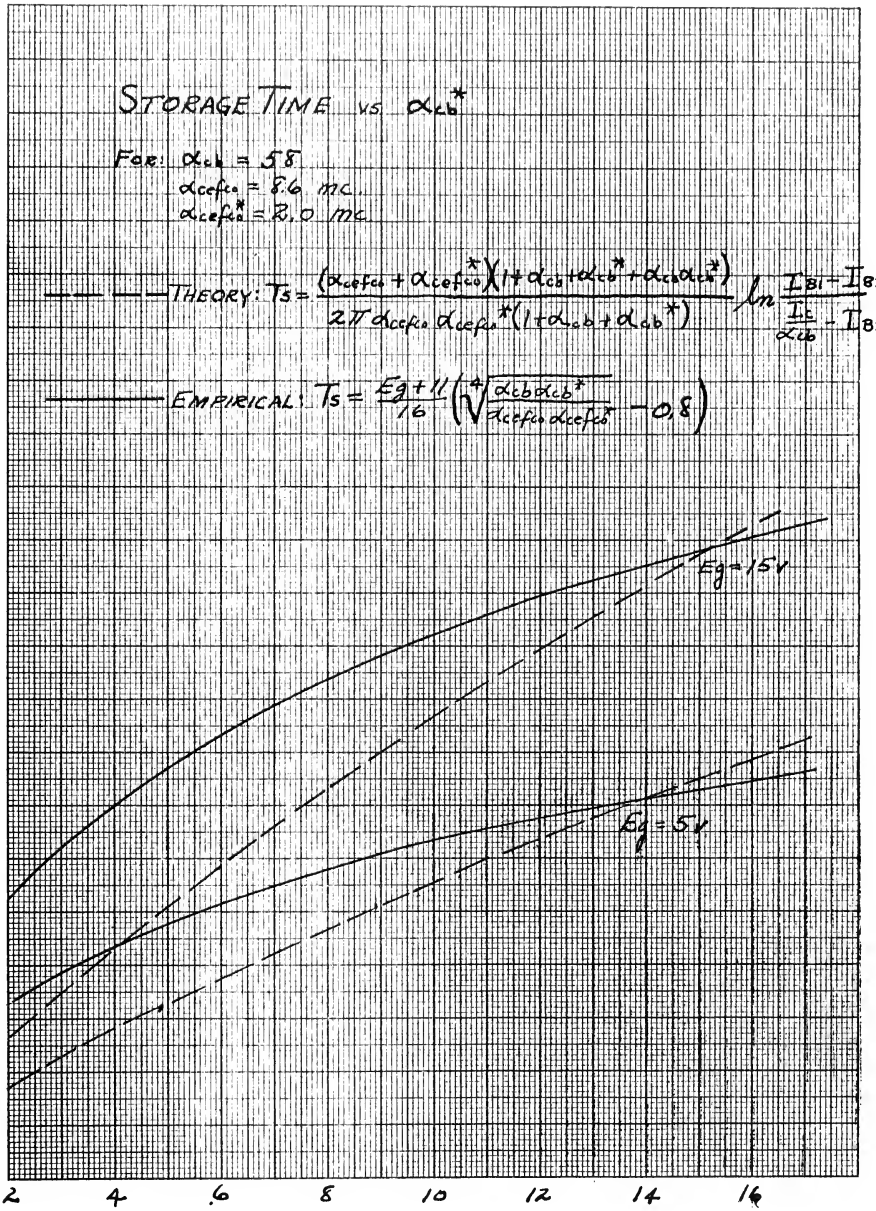
STORAGE TIME vs α_{cb}^*
For: $\alpha_{cb} = .58$
$\alpha_{ceFco} = 8.6$ mc
$\alpha_{ceFco}^* = 2.0$ mc
THEORY: $T_S = \frac{(\alpha_{ceFco} + \alpha_{ceFco}^*)(1+\alpha_{cb}+\alpha_{cb}^*+\alpha_{cb}\alpha_{cb}^*)}{2\pi\alpha_{ceFco}\alpha_{ceFco}^*(1+\alpha_{cb}+\alpha_{cb}^*)} \ln \frac{I_{B1}-I_{B2}}{\frac{I_C}{\alpha_{cb}}-I_{B2}}$
EMPIRICAL: $T_S = \frac{Eg+11}{16}\left(\sqrt[4]{\frac{\alpha_{cb}\alpha_{cb}^*}{\alpha_{ceFco}\alpha_{ceFco}^*}} - 0.8\right)$
Eg = 15 v
Eg = 5 v
3
2
1
2
4
6
8
10
12
14
16
$\alpha_{cb(1)}^*$

Fig. 33

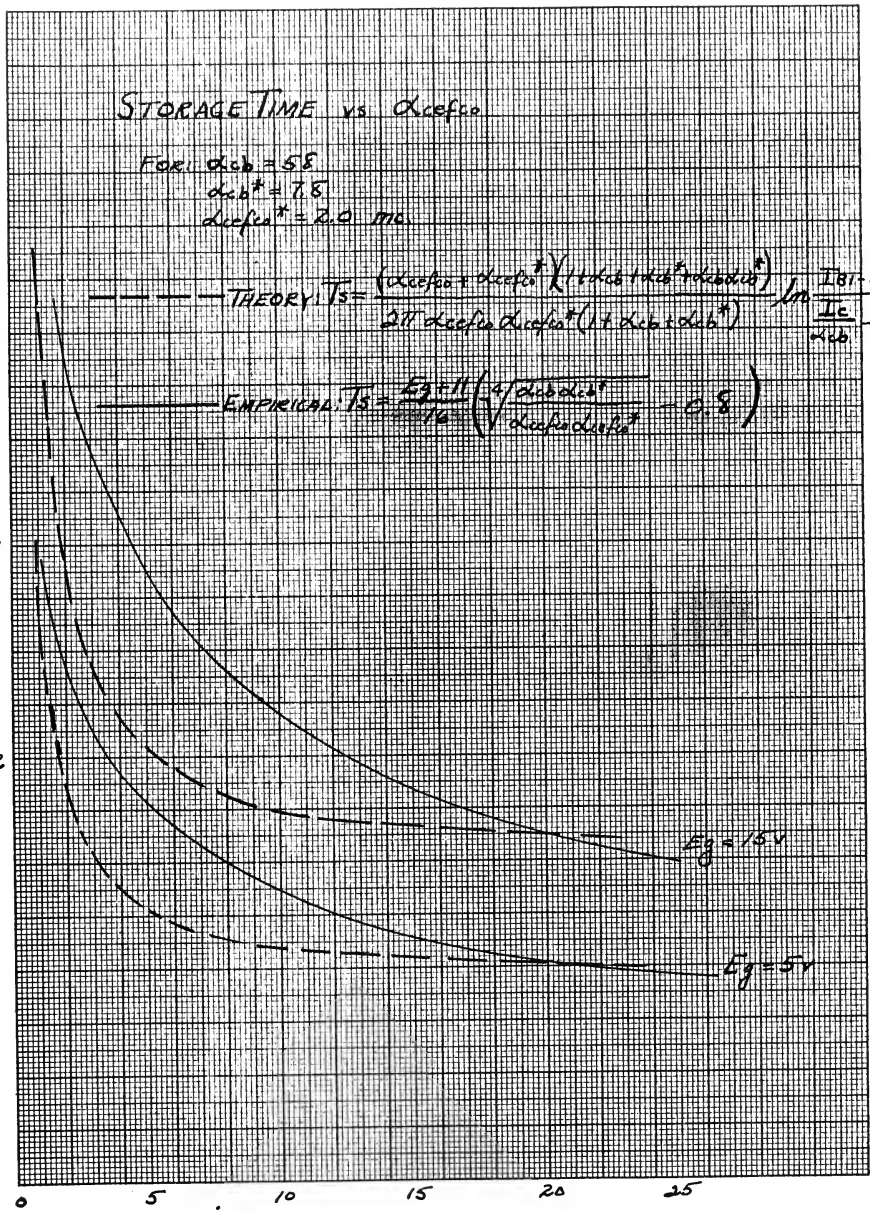

Fig. 34 α_{cefco} IN mc.

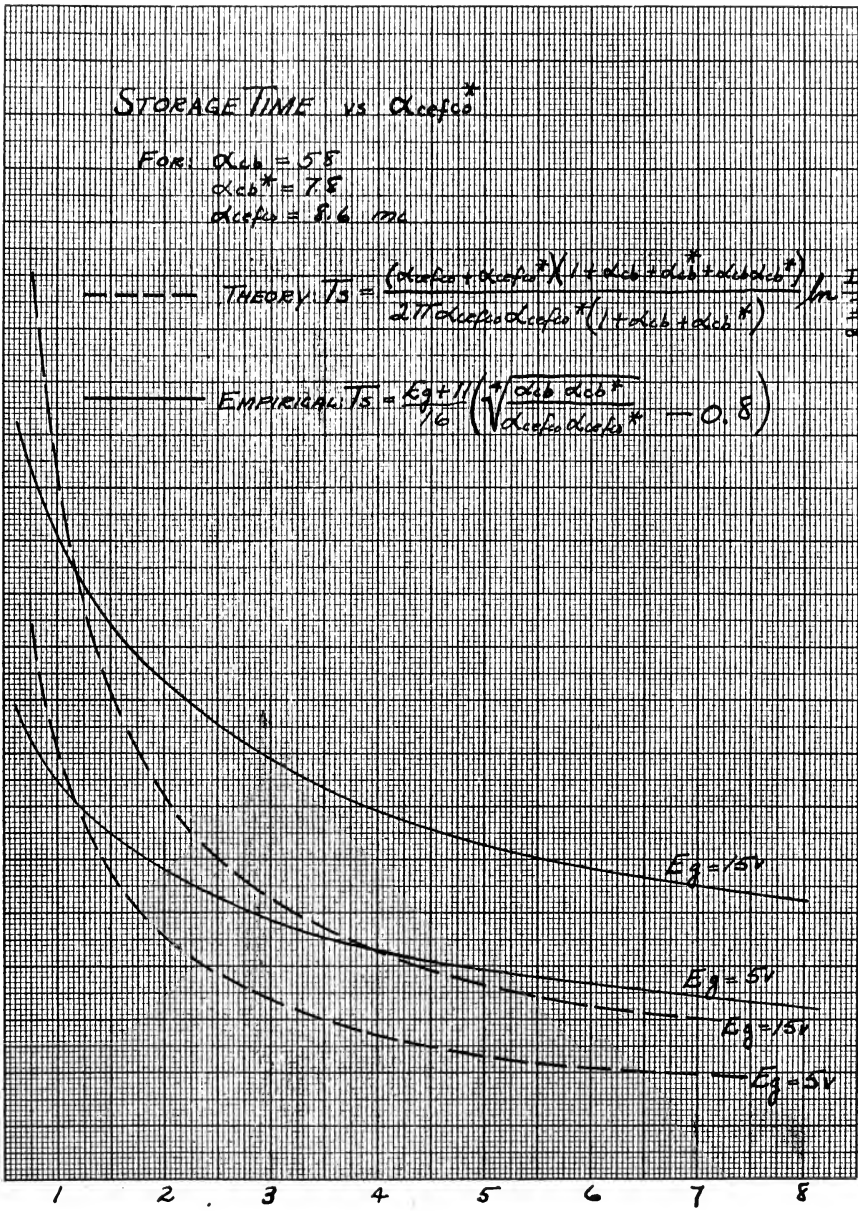
STORAGE TIME vs α_{cefco}^*
FOR: $\alpha_{cb} = 58$
$\alpha_{cb}^* = 7.8$
$\alpha_{cefco} = 8.6$ mc
THEORY: $T_s = \frac{(\alpha_{cefco} + \alpha_{cefco}^*)(1 + \alpha_{cb} + \alpha_{cb}^* + \alpha_{cb}\alpha_{cb}^*)}{2\pi\alpha_{cefco}\alpha_{cefco}^*(1 + \alpha_{cb} + \alpha_{cb}^*)} \ln \frac{I_{B1} - I_{B2}}{\frac{I_c}{\alpha_{cb}} - I_{B2}}$
EMPIRICAL: $T_s = \frac{E_g + 11}{16}\left(\sqrt{\frac{\alpha_{cb}\alpha_{cb}^*}{\alpha_{cefco}\alpha_{cefco}^*}} - 0.8\right)$
T_s IN μS
E_g=15V
E_g=5V
E_g=15V
E_g=5V
α_{cefco}^* IN mc.

Fig. 35

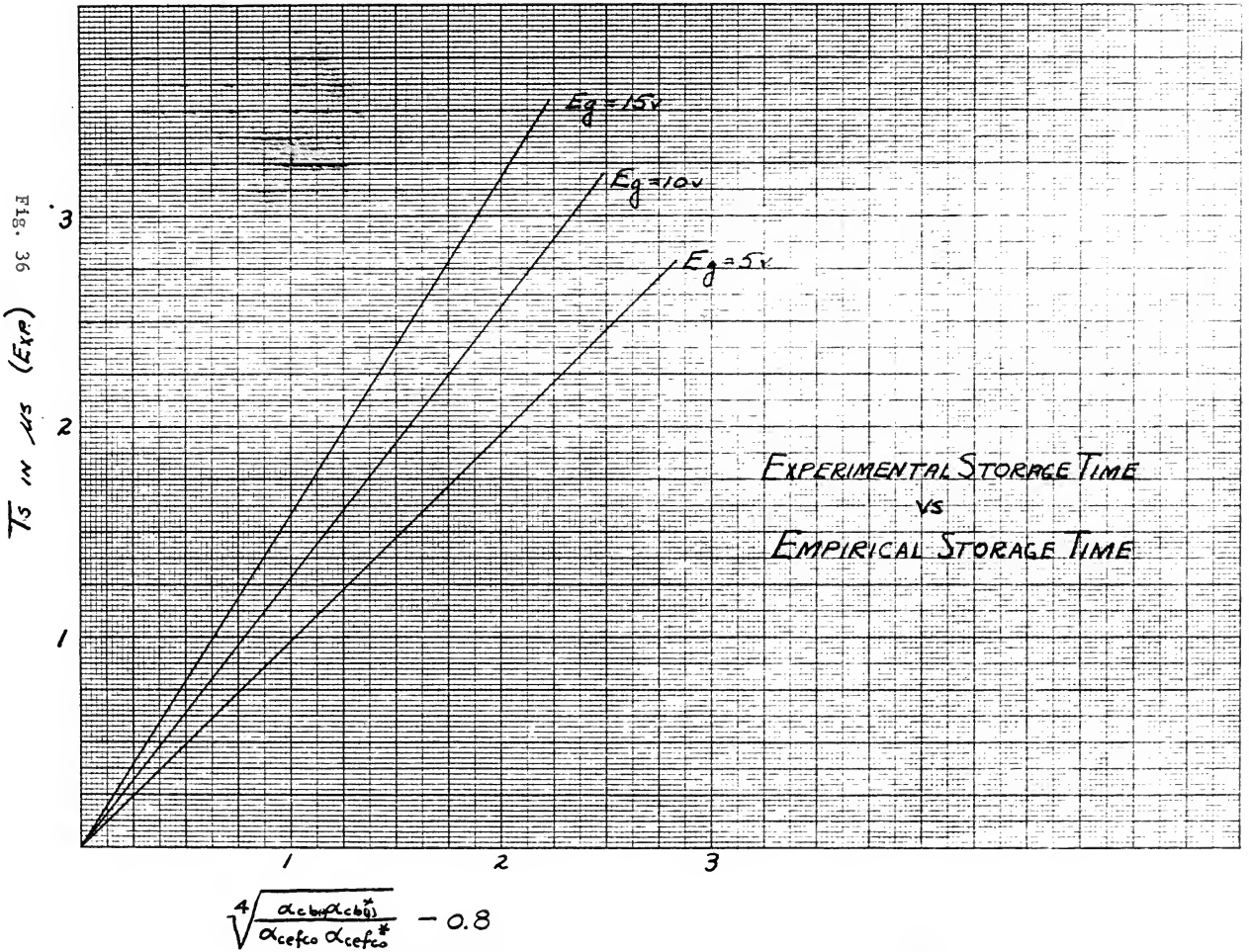
$E_g = 15v$
$E_g = 10v$
$E_g = 5v$
EXPERIMENTAL STORAGE TIME
VS
EMPIRICAL STORAGE TIME
T_S IN μs (EXP)
1
2
3
$\sqrt[4]{\frac{\alpha_{cbo}\alpha_{cb(j)}^{*}}{\alpha_{cefco}\alpha_{cefco}^{*}}} - 0.8$

Fig. 36

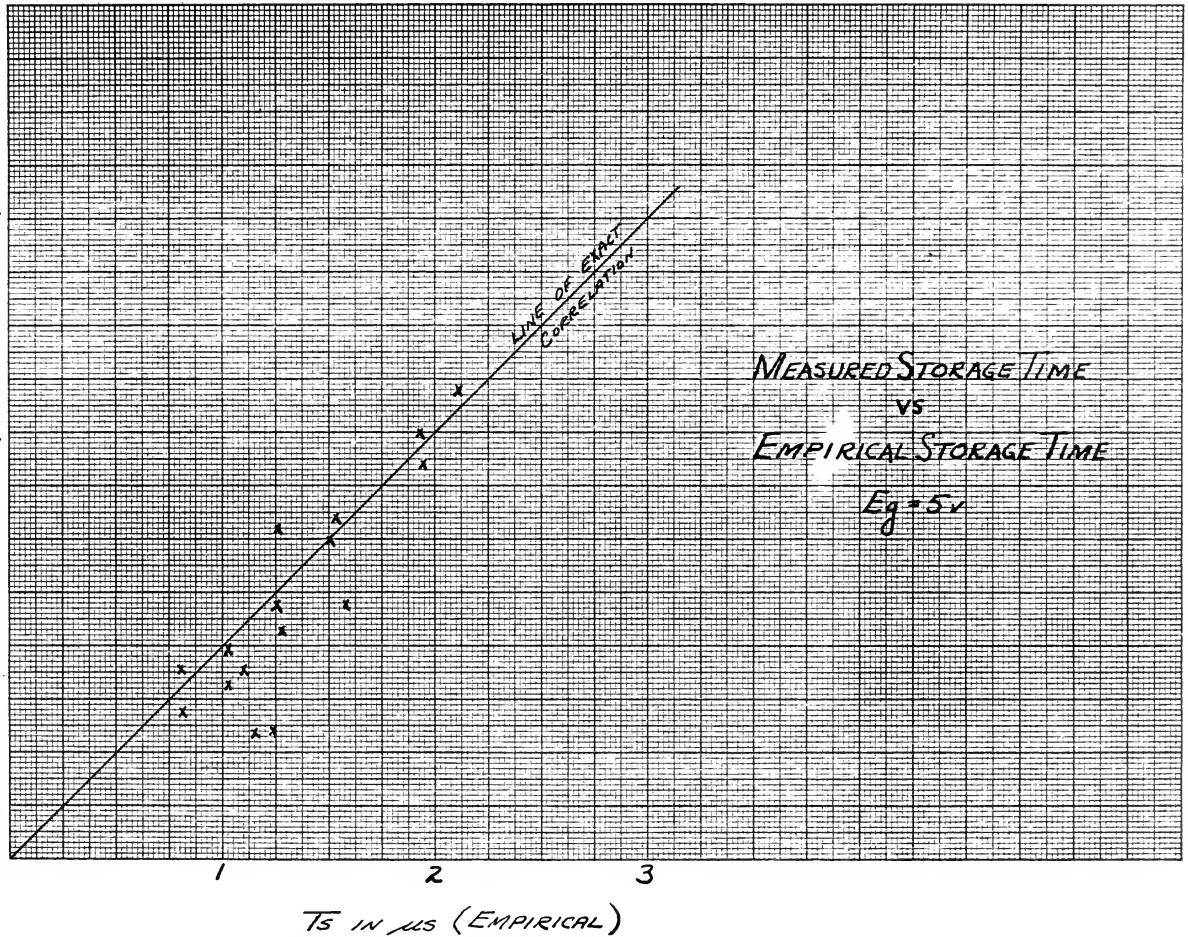
LINE OF EXACT CORRELATION
MEASURED STORAGE TIME
VS
EMPIRICAL STORAGE TIME
Eq - 5v
TS IN μs (EXPERIMENTAL)
TS IN μs (EMPIRICAL)
1
2
3

Fig. 37

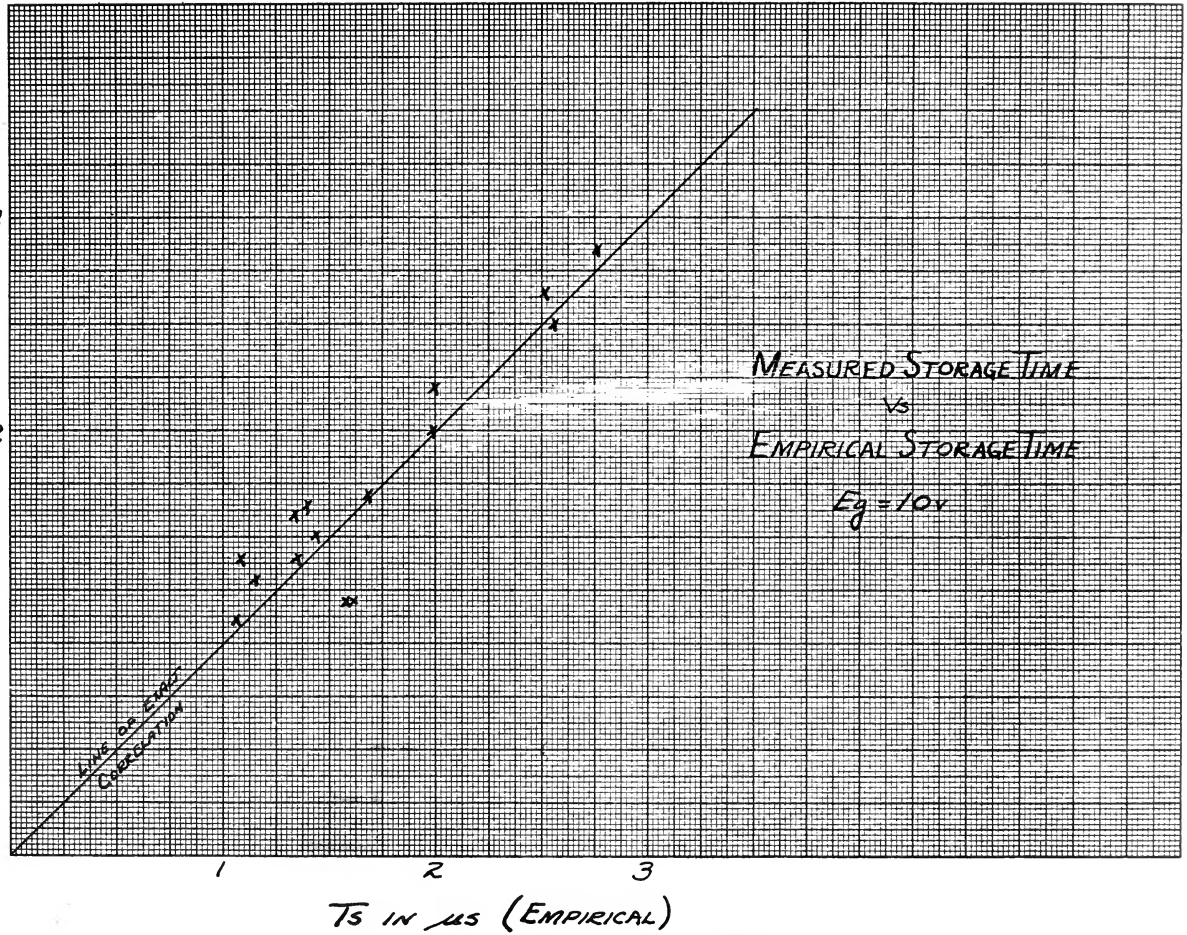
MEASURED STORAGE TIME
VS
EMPIRICAL STORAGE TIME
$E_g = 10v$
LINE OF EXACT CORRELATION
T_S IN μs (EXPERIMENTAL)
T_S IN μs (EMPIRICAL)
1
2
3

Fig. 38

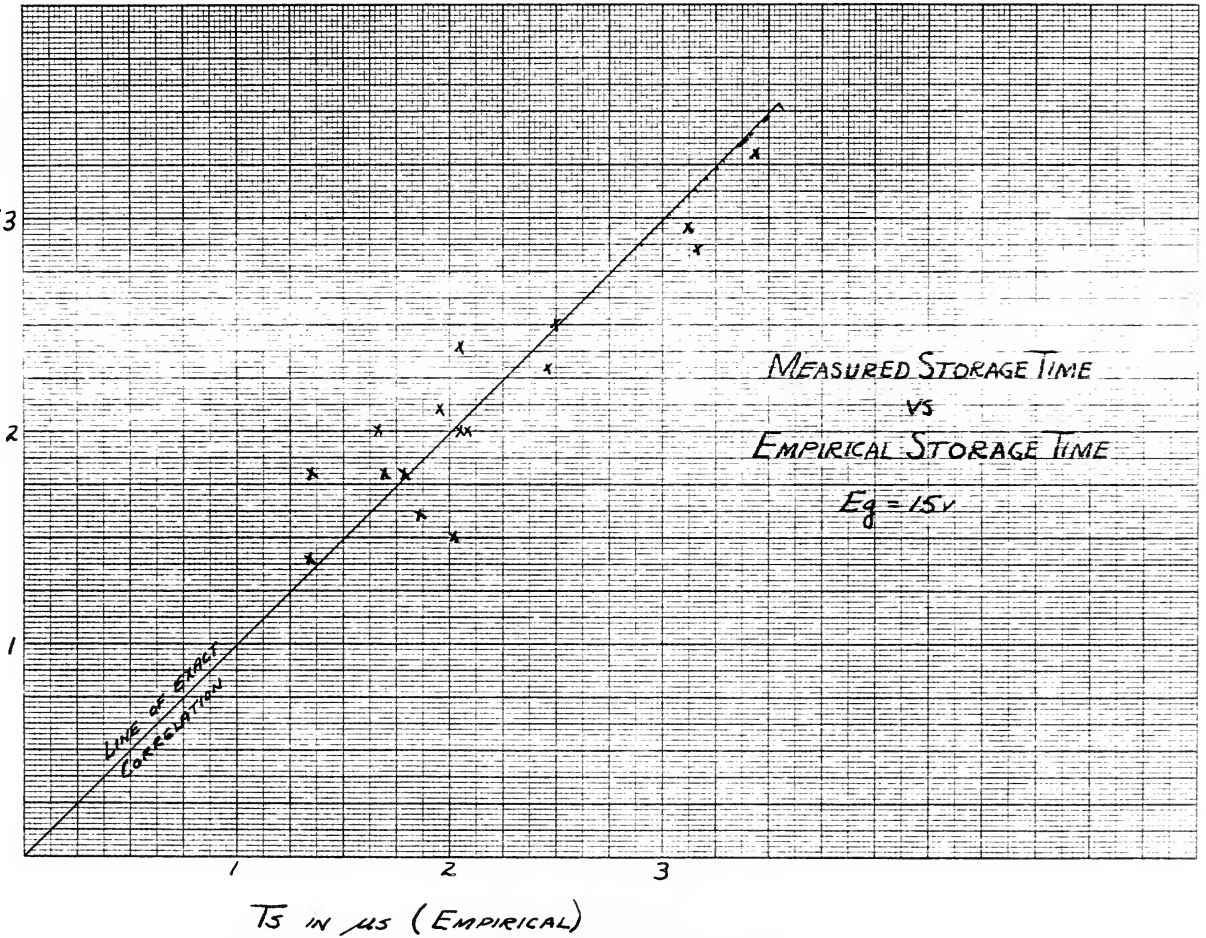
MEASURED STORAGE TIME
VS
EMPIRICAL STORAGE TIME
$E_{g_0} = 15V$
LINE OF EXACT CORRELATION
T_S IN μs (EXPERIMENTAL)
T_S IN μs (EMPIRICAL)
1
2
3

Fig. 39

results show better correlation than those using the theory for the method used in measuring the storage time. It also should be remembered that this empirical equation is for the particular test circuit in use. However, changing the external circuit parameters, within reason of course, for a constant current drive should result in only changing the constants of the equation. Thus, the storage time is approximately a function of $\sqrt[4]{\frac{\alpha_{cb}\alpha_{cb}^{*}}{\alpha_{cefco}\alpha_{cefco}^{*}}}$

CHAPTER V

CONCLUSIONS

1. A Discussion of Results

The experimental results have shown that using a circuit with a constant current (high impedance) generator driving the unit into the saturation regions, $r_{bb'}$, C_e, and the pulse repetition rate will have no affect on the switching times, as long as $r_{bb'} \ll R_g$ and $C_e \ll \omega_{ce} R_L C_{b'c}$, as will almost always be the case. If $r_{bb'}$ is not much less than R_g, we no longer have a constant current generator. If C_e is not much less than $\omega_{ce} R_L C_{b'c}$ it must be added to $\omega_{ce} R_L C_{b'c}$ and will cause an increase in the rise and fall times.

It has been demonstrated that the equations of Moll (2) modified to include the feedback capacitance and the factor of K, which occurs when converting from ω_{ce} to ω_{cb}, will give calculated values which agree within about 20% of the experimental values.

From these equations it can be seen that increasing the value of $\omega_{ce} R_L C_{b'c}/K$ will increase the effect of the feedback capacitance and thus increase the rise and fall times. It is thus important to keep $C_{b'c}$ as low as possible.

The effects of the α_{cb} and ω_{ce} parameters, forward and inverse, can best be summarized in the following chart:

	T_r	T_f	T_s
Decreasing α_{cb}	Increases slightly	Decreases	Decreases
Increasing ω_{ce}	Decreases	Decreases	Decreases
Decreasing α_{cb}*	---	---	Decreases
Increasing ω_{ce}*	---	---	Decreases

The effects indicated for ω_{ce} will hold as long as $\omega_{ce}C_{b'c}R_L/K < 1$. When $\omega_{ce}C_{b'c}R_L/K > 1$, increasing ω_{ce} will not improve the rise and fall times, but the storage time will continue to decrease.

The effect of decreasing the temperature is to decrease the fall and storage times with little change in the rise time.

Thus, for the fastest rise and fall times, and the shortest storage times the value of $C_{b'c}$ must be kept at a minimum, α_{cb} should be no larger than is necessary to give the required gain, and ω_{ce} should be as high as possible. Cooler temperatures improve transient times also.

2. General

It is obvious that compared with vacuum tubes, transistors of the type used to obtain the results of this paper, have slower switching times. A typical switching time for a vacuum tube, when the tube is the limiting element, may be in the order of 0.1 us or less. Driving a transistor into saturation, rise times of this order can be approached. The time for a transistor to return to the OFF state after the input signal is removed is, however, considerably longer than the time for the vacuum tube to respond. In addition, transistors are subject to storage times which vacuum tubes are not.

Even though transistors are presently slower than vacuum tubes, they have so many other advantages, especially in computer and other automatic

control applications, that their use is becoming more common every day. The ever increasing efforts to increase the frequency response and decrease the times of switching is resulting in better units and their use in the future may completely replace the vacuum tube in the computer and automatic control equipments.

BIBLIOGRAPHY

1. Ebers, J. J. and Moll, J. L. — LARGE-SIGNAL BEHAVIOR OF JUNCTION TRANSISTORS
Proc. I.R.E., Vol. 42, No. 12
pp 1761-1772, December 1954

2. Moll, J. L. — LARGE-SIGNAL TRANSIENT RESPONSE OF JUNCTION TRANSISTORS
Proc. I.R.E., Vol. 42, No. 12
pp 1773-1784, December 1954

3. Deuitch, D. E. — JUNCTION TRANSISTOR SWITCHING CIRCUIT DESIGN
Unpublished report of R.C.A.
October 1955

4. Anderson, A. E. — TRANSISTORS IN SWITCHING CIRCUITS
Proc. I.R.E., Vol. 40, No. 11
pp 1541-1558, November 1952

5. Giacoletto, L. J. — STUDY OF P-N-P ALLOY JUNCTION TRANSISTORS FROM D-C THROUGH MEDIUM FREQUENCIES
R.C.A. Review, Vol. XV, No. 4
pp 506-562, December 1954

6. Lo, A. W., et.al. — TRANSISTOR ELECTRONICS
Prentice-Hall, 1955

7. Saby, J. S. — FUSED IMPURITY P-N-P JUNCTION TRANSISTORS
Proc. I.R.E., Vol. 40, No. 11
pp 1358-1364, November 1952

8. Eshelman, C. R. — THE VARIATION OF TRANSISTOR PARAMETERS
Unpublished report of R.C.A.
December 1955

9. Pritchard, R. L. — FREQUENCY VARIATIONS OF CURRENT-AMPLIFICATION FACTOR FOR JUNCTION TRANSISTORS
Proc. I.R.E., Vol. 40, No. 11
pp 1476-1481, November 1952

10. Pritchard, R. L. — FREQUENCY VARIATIONS OF JUNCTION TRANSISTOR PARAMETERS
Proc. I.R.E., Vol. 42, No. 5
pp 786-799, May 1954

11. Shea, R. F. — PRINCIPLES OF TRANSISTOR CIRCUITS
John Wiley and Sons, Inc., 1953

12. Haneman, D. — EXPRESSION FOR THE "α CUT-OFF" FREQUENCY IN JUNCTION TRANSISTORS
Proc. I.R.E., Vol. 42, No. 12
pp 1808-1809, December 1954

13. Giacoletto, L. J. — COMPARISON OF α_{cb} AND α_{ce} CUTOFF
Special Unpublished Notes.
R.C.A., March 1956

TRANSISTOR CHARACTERISTICS

Unit	No.	α_{cb} 6V, 1 ma.	r_{eb}*	α_{eb} 6V, 5 ma.	r_{cb}*	$r_{ce(fb)}$	$r_{ce(fc)}$*	$\alpha_{ce(sat)}$
						meg.		
K6-12	1	25.8	13.8	31.5	15.4	6.9	4.3	165
K8-13	2	76	7.2	197	8.75	8.5	2.35	92
-34	3	32	16.1	40.5	19.0	10.2	6.2	210
K9-4	4	36.5	7.75	42.8	9.1	8.35	2.5	158
-12	5	22.4	12.3	29	13.5	8.3	4.6	140
K11-12	6	46.5	9.4	55	10.3	8.05	2.56	79
-19	7	93.5	7.6	130	8.6	10.0	2.25	84
-32	8	20.2	7.2	22.6	7.5	6.1	1.3	134
K16A-20	9	62	6.7	81	7.3	7.15	1.01	90
-23	10	24	6.1	26.4	6.45	6.55	.78	180
K31-3	11	40	9.35	57	10.8	7.65	2.86	131
-9	12	38.5	12.9	46	7.3	9.5	4.45	170
CV-97	13	30.5	5.8	39.5	6.9	6.15	1.5	152
-98	14	56.8	5.85	68	6.55	6.1	.76	84
-100	15	23	11.1	26	13	6.7	2.5	190
-102	16	53.5	4.45	55.5	4.9	6.35	.80	139
-103	17	70.5	4.7	85	4.8	6.1	.64	87.9
K18-9	18	55.5	5.0	66	5.6	6.95	.70	110.5
-14	19	78.5	7.35	96	7.95	12.1	1.75	129.5
-18	20	99	6.4	126	7.1	8.4	1.3	75
K19-18	21	88.5	7.45	109	8.0	5.8	1.48	59.5
-20	22	87	4.0	99	3.45	6.8	.68	40
K20-1	23	61.5	5.2	80	5.7	5.0	.75	66.5
-30	24	106.7	7.1	166	8.1	20.4	1.96	143.5
-17	25	84.5	7.65	106	9.0	6.5	1.64	68
K22-16	26	51	5.7	69	6.7	4.9	.99	73
19	27	49.5	7.0	58	8.2	8.2	2.21	140.5
K189-16	28	60.5	3.0	59.5	2.8	2.35	.291	45.8
-17	29	45.5	4.95	46	5.2	1.7	.36	44.3
-18	30	52.5	3.0	55	3.4	2.13	1.04	16.8
K190-13	31	48	3.6	47	3.6	2.18	.295	53.5
-17	32	76	3.85	73.5	3.55	3.35	.415	54.5
-22	33	39	2.65	39	2.4	1.63	.2	47.3
K5-35	34	53.5	5.6	56.5	5.75	3.35	.89	63
K6-30	35	62	4.9	64.5	4.8	3.4	.68	59
-33	36	104	5.65	116	5.7	4.7	.66	45.8

* Indicates inverse readings
* See text to read

Unit	No.	CoIc -12V	CoIe -12V	CoVc -20V	CoVe -20V	rbb'	Cc	Ce	2Ve	2Ic	2Ce	
K6-12	1	0.5	6.1	38	20	77	8.1	7.7	.08	0.98	.172	
K8-12	2	0.6	0.5	52	34	75	11.1	7.4	.09	0.98	.200	
-34	3	0.35	1.6	49	26	79	10.0	9.0	.08	0.98	.095	
K9-4	4	0.4	0.6	43	32	73	10.5	7.5	.08	1.0	.240	
-12	5	0.4	0.4	48	30	75	9.8	8.3	.08	0.98	.119	
K11-12	6	0.45	5.3	42	20	80	11.0	7.9	.08	1.0	.305	
-19	7	0.4	0.4	43	28	83	11.1	7.0	.10	1.05	.250	
-32	8	0.45	0.5	44	36	75	10.8	6.8	.08	0.98	.072	
K16A-20	9	0.5	0.6	60	57	81	10.5	6.2	.08	0.99	.094	
-23	10	0.8	0.6	56	49	82	10.0	5.9	.08	0.97	.296	
K31-3	11	0.7	0.75	43	46	81	9.0	7.4	.06	0.98	.102	
-9	12	0.45	0.9	38	30	77	8.9	7.6	.09	0.99	.082	
CV-97	13	0.7	2.9	48	20	70	9.6	5.5	.07	0.98	.116	
-98	14	2.24	0.55	24	40	87	11.0	4.5	.09	0.99	.104	
-100	15	0.65	0.9	50	36	86	7.8	4.9	.07	0.97	.023	
-102	16	0.75	0.5	41	34	79	12.1	5.1	.08	1.0	.132	
-103	17	0.8	6.02	30	66	95	10.2	4.1	.09	0.99	.100	
R18-9	18	3.4	0.5	50	47	93	10.9		.09	1.0	0.11	0.38
-14	19	0.5	0.4	49	53	108	9.6		.10	0.99	0.08	0.29
-18	20	0.7	0.55	42	60	110	9.9		.10	0.99	0.08	0.225
R19-18	21	0.7	1.3	41	33	94	9.2		.07	0.98	0.08	0.242
-20	22	1.0	1.74	45	29	122	10.8		.10	0.99	0.11	0.200
R20-1	23	0.75	0.55	62	51	85	11.0		.09	0.98	0.10	0.32
-10	24	0.70	0.55	60	57	158	10.9		.09	1.0	0.08	0.178
-17	25	0.75	2.61	46	24	93	11.9		.09	0.99	0.08	0.265
R22-16	26	0.5	0.4	46	26	59	11.1		.08	1.0	0.09	0.36
-19	27	0.3	0.55	39	38	66	10.9		.08	1.02	0.08	0.14
E18-16	28	2.0	0.5	27	43	90	11.1	4.2	.09	0.98	0.24	0.10
-17	29	1.0	0.35	28	34	55	12.0	6.9	.08	0.98	0.12	0.53
-18	30	2.2	0.3	29	37	110	8.7	6.3	.09	0.99	0.11	0.15
E19-13	31	0.45	3.45	44	20	51	14.0	6.1	.08	0.98	0.12	0.50
-17	32	1.7	0.4	30	36	128	11.0	3.9	.10	0.98	0.13	0.35
-22	33	1.5	0.55	29	35	64	12.2	4.6	.07	0.97	0.15	0.63
K5-35	34	0.4	0.5	49	31	58	11.4	6.5	.09	0.99	0.11	0.49
K6-30	35	0.9	1.8	31	27	57	11.6	5.9	.09	0.98	0.11	0.38
-33	36	0.6	0.9	50	35	74	13.0	5.8	.10	0.99	0.09	0.21

Thesis
J215 Jackson 23967
A study of the parameters controlling the switching times of a junction transistor operating in the saturated region.